9. Daiki Omata Ryo Suzuki, Yusuke Oda, Yoshikazu Sawaguchi, Yoichi Negishi, Kazuo Maruyama, Selective gene delivery for brain by bubble liposomes and ultrasound, Tht 5th Asian Arden Conference, 名古屋、2013 年 8 月 5-6 日
10. 小俣大樹、鈴木　亮、小田雄介、澤口能一、宇留賀仁史、関むつみ、直井智幸、根岸洋一、丸山一雄、バブルリポソームと超音波を利用した肝臓選択的な遺伝子導入、第 57 回日本薬学会関東支部大会、東京、2013 年 10 月 26 日
11. 小沼俊也、鈴木　亮、小俣大樹、小田雄介、澤口能一、宇留賀仁史、関むつみ、直井智幸、根岸洋一、丸山一雄、バブルリポソームと超音波による脳標的型遺伝子デリバリーシステム、第 57 回日本薬学会関東支部大会、東京、2013 年 10 月 26 日
12. 小田雄介、鈴木　亮、関むつみ、澤口能一、小俣大樹、宇留賀仁史、岡田直貴、中川晋作、丸山一雄、バブルリポソームと超音波により抗原送達した樹状細胞ワクチンによるがん転移予防効果、第 57 回日本薬学会関東支部大会、東京、2013 年 10 月 26 日
13. 関むつみ、小田雄介、鈴木　亮、小俣大樹、澤口能一、宇留賀仁史、岡田直貴、中川晋作、丸山一雄、がん免疫療法における樹状細胞への抗原送達に向けた新たな戦略、第 57 回日本薬学会関東支部大会、東京、2013 年 10 月 26 日
14. 宇留賀仁史、鈴木　亮、小俣大樹、小田雄介、関むつみ、澤口能一、根岸洋一、岡田直貴、中川晋作、丸山一雄、バブルリポソームと超音波を用いたサイトカイン発現遺伝子導入による癌治療効果、第 57 回日本薬学会関東支部大会、東京、2013 年 10 月 26 日

H. 知的財産権の出願・登録状況

H-1 特許取得

なし

H-2 実用新案登録

なし

H-3 その他

なし

I. 研究協力者

小俣　大樹
小田　雄介
平田　圭一
宇留賀　仁史
関　むつみ

研究成果の刊行に関する一覧表

書籍

著者氏名	論文タイトル名	書籍全体の編集者名	書　籍　名	出版社名	出版地	出版年	ページ
	該当事項なし						

雑誌

発表者氏名	論文タイトル名	発表誌名	巻号	ページ	出版年
Li X., Saeki R., Watari A., Yagi K., Kondoh M.	Tissue distribution and safety evaluation of a claudin-targeting molecule, the C-terminal fragment of Clostridium perfringens enterotoxin.	*Eur. J. Pharm. Sci.*	14(52)	132-7	2014
Iida M., Yoshida T., Watari A., Yagi K., Hamakubo T., Kondoh M.	A baculoviral display system to assay viral entry.	*Biol. Pharm. Bull.*	36(11)	1867-9	2013
Sugano M., Negishi Y., Endo Takahashi Y., Hamano N., Usui M., Suzuki R., Maruyama K., Aramaki Y., Yamamoto M.	Gene delivery to periodontal tissue using Bubble liposomes and ultrasound.	*J. Periodontal Res.*			2013
Hagisawa K., Nishioka T., Suzuki R., Maruyama K., Takase B., Ishihara M., Kurita A., Yoshimoto N., Nishida Y., Iida K., Luo H., Siegel RJ.	Thrombus-targeted perfluorocarbon-containing liposomal bubbles for enhancement of ultrasonic thrombolysis: in vitro and in vivo study.	*J Thromb Haemost.*	11(8)	1565-73	2013

Negishi Y., Tsunoda Y., Hamano N., Omata D., EndoTakahashi Y., Suzuki R., Maruyama K., Nomizu M., Aramaki Y.	Ultrasound-mediated gene delivery systems by AG73-modified bubble liposomes.	*Biopolymers.*	100(4)	402-7	2013
EndoTakahashi Y., Negishi Y., Nakamura A., Suzuki D., Ukai S., Sugimoto K., Moriyasu F., Takagi N., Suzuki R., Maruyama K, Aramaki Y.	pDNA-loaded Bubble liposomes as potential ultrasound imaging and gene delivery agents.	*Biomaterials.*	34(11)	2807-13	2013
Hamano N., Negishi Y., Omata D., Takahashi Y., Manandhar M., Suzuki R., Maruyama K., Nomizu M., Aramaki Y.	Bubble liposomes and ultrasound enhance the antitumor effects of AG73 liposomes encapsulating antitumor agents.	*Mol. Pharm.*	10(2)	774-9	2013
Negishi Y., Hamano N., Tsunoda Y., Oda Y., Choijamts B., EndoTakahashi Y., Omata D., Suzuki R., Maruyama K., Nomizu M., Emoto M., Aramaki Y.	AG73-modified Bubble liposomes for targeted ultrasound imaging of tumor neovasculature.	*Biomaterials.*	34(2)	501-7	2013

European Journal of Pharmaceutical Sciences xxx (2013) xxx–xxx

Contents lists available at ScienceDirect

European Journal of Pharmaceutical Sciences

journal homepage: www.elsevier.com/locate/ejps

Tissue distribution and safety evaluation of a claudin-targeting molecule, the C-terminal fragment of *Clostridium perfringens* enterotoxin

Xiangru Li, Rie Saeki, Akihiro Watari, Kiyohito Yagi, Masuo Kondoh *

Laboratory of Bio-Functional Molecular Chemistry, Graduate School of Pharmaceutical Sciences, Osaka University, Suita, Osaka 565-0871, Japan

ARTICLE INFO

Article history:
Received 2 April 2013
Received in revised form 25 October 2013
Accepted 25 October 2013
Available online xxxx

Keywords:
Claudin
Clostridium perfringens enterotoxin
Kidney
Liver
Tissue distribution

ABSTRACT

We previously found that claudin (CL) is a potent target for cancer therapy using a CL-3 and -4-targeting molecule, namely the C-terminal fragment of *Clostridium perfringens* enterotoxin (C-CPE). Although CL-3 and -4 are expressed in various normal tissues, the safety of this CL-targeting strategy has never been investigated. Here, we evaluated the tissue distribution of C-CPE in mice. Ten minutes after intravenous injection into mice, C-CPE was distributed to the liver and kidney (24.0% and 9.5% of the injected dose, respectively). The hepatic level gradually fell to 3.2% of the injected dose by 3 h post-injection, whereas the renal C-CPE level gradually rose to 46.5% of the injected dose by 6 h post-injection and then decreased. A C-CPE mutant protein lacking the ability to bind CL accumulated in the liver to a much lesser extent (2.0% of the dose at 10 min post-injection) than did C-CPE, but its renal profile was similar to that of C-CPE. To investigate the acute toxicity of CL-targeted toxin, we intravenously administered C-CPE-fused protein synthesis inhibitory factor to mice. The CL-targeted toxin dose-dependently increased the levels of serum biomarkers of liver injury, but not of kidney injury. Histological examination confirmed that injection of CL-targeted toxin injured the liver but not the kidney. These results indicate that potential adverse hepatic effects should be considered in C-CPE-based cancer therapy.

1. Introduction

Most lethal cancers are derived from epithelial tissues (Jemal et al., 2008), and many therapeutic strategies targeting such cancers have been developed. Selective delivery of anti-cancer agents to cancer cells is a popular anti-cancer strategy (Adair et al., 2012; Yewale et al., 2013). Many membrane proteins that are present at much higher levels in cancer cells than in normal cells have been identified. Antibodies have recently become available as anti-cancer drugs targeting breast cancer (pertuzumab, directed against human epidermal growth factor receptor-2) and colon cancer (panitumumab, directed against epidermal growth factor receptor) (Dent et al., 2013; Zouhairi et al., 2011).

Normal epithelial cells develop complex intercellular tight junctions (TJs) that prevent the free movement of solutes across epithelial cell sheets and of membrane proteins and lipids between apical and basolateral membranes (Furuse and Tsukita, 2006; Rodriguez-Boulan and Nelson, 1989; Vermeer et al., 2003). In contrast, TJ functionality is frequently abnormal in transformed epithelial cells. As a result, cellular polarity and intercellular contact are often lost, both in the early stages of carcinogenesis and in advanced tumors (Wodarz and Nathke, 2007). Such findings indicate that the membrane proteins of TJs, which are difficult to access in normal epithelia but are exposed in malignant cells, may be candidate targets for cancer therapy.

Freeze-fracture replica electron microscopy has shown that TJs present as a series of continuous, anastomotic, intramembranous particulate strands, or fibrils (Farquhar and Palade, 1963; Staehelin, 1973). The TJ-containing strands are composed of both intracellular and integral membrane proteins, including claudin (CL) (Anderson and Van Itallie, 2009). CL comprises a tetraspan protein family with 27 members (Mineta et al., 2011). Interestingly, the expression of CL-3 or -4, or both, is increased in breast, gastric, intestinal, ovarian, pancreatic, and prostatic carcinomas (Singh et al., 2010; Tsukita et al., 2008; Turksen and Troy, 2011).

Clostridium perfringens enterotoxin (CPE) causes food poisoning in humans (McClane and Chakrabarti, 2004). CL-3 and CL-4 serve as receptors for CPE, and CPE is cytotoxic to cells expressing these CLs (Long et al., 2001; Sonoda et al., 1999). Intratumoral administration of CPE attenuates pancreatic tumor growth, and intraperitoneal administration of CPE inhibits ovarian tumor growth

Abbreviations: ALT, alanine aminotransferase; AST, aspartate aminotransferase; BSA, bovine serum albumin; BUN, blood urea nitrogen; CL, claudin; CPE, *Clostridium perfringens* enterotoxin; C-CPE, C-terminal fragment of CPE; FACS, fluorescence-activated cell sorter; PBS, phosphate-buffered saline; PSIF, protein synthesis inhibitory factor; TJ, tight junction.

* Corresponding author. Tel.: +81 6 6879 8196; fax: +81 6 6879 8199.
E-mail address: masuo@phs.osaka-u.ac.jp (M. Kondoh).

0928-0987/$ - see front matter © 2013 Published by Elsevier B.V.
http://dx.doi.org/10.1016/j.ejps.2013.10.018

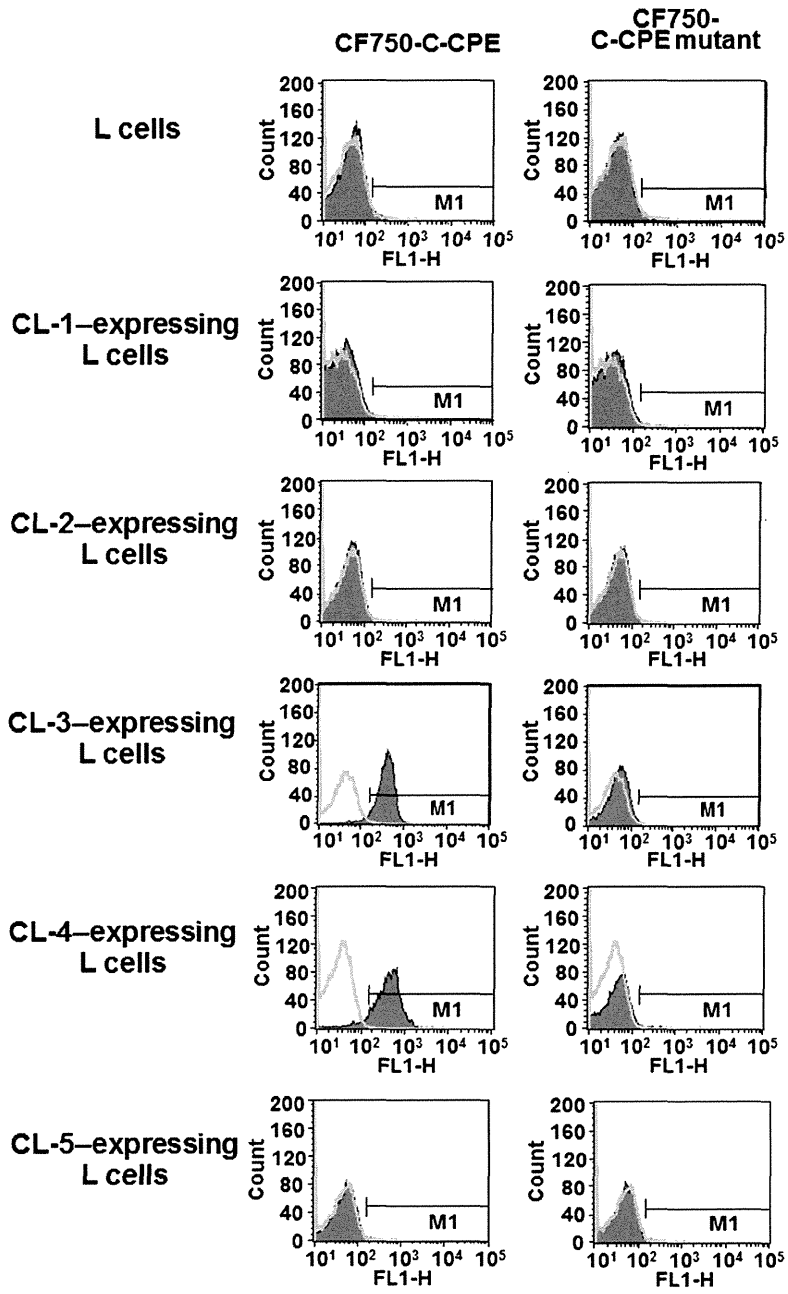

Fig. 1. Flow cytometric analysis of the interaction of claudins (CLs) with the CF750-labeled C-terminal fragment of *Clostridium perfringens* enterotoxin (C-CPE). Mouse fibroblast L cells were incubated with 10 μg/ml CF750-labeled C-CPE or a mutant form of C-CPE (also labeled with CF750) for 1 h and then subjected to fluorescence-activated cell sorter analysis as described in the Materials and Methods. Unfilled curves show the results obtained when cells were not treated with C-CPE proteins. Filled curves show data from C-CPE-treated cells. FL1-H indicates fluorescent intensity and M1 indicates C-CPE-bound cells.

(Michl et al., 2001; Santin et al., 2005). Moreover, the C-terminal fragment of CPE (C-CPE) is a ligand of CL-3 and CL-4 (Sonoda et al., 1999). We previously prepared a CL-targeting cytotoxic molecule via fusion of C-CPE and a protein synthesis inhibitory factor (PSIF) derived from *Pseudomonas* exotoxin (Ebihara et al., 2006). We found that intratumoral or intravenous administration of C-CPE-fused PSIF attenuated the growth of murine breast cancer cells (Saeki et al., 2009, 2010). Thus, drugs that include all or part of CPE may be useful for targeting CLs in cancer therapy.

CLs are expressed throughout the body. Evaluation of the possible adverse effects of CL-targeting molecules is critical if the CPE technology described above is to be used for cancer therapy. However, no such hazard assessment has been performed to date. Here, we investigated the tissue distribution of C-CPE and the tissue injury caused by C-CPE-fused PSIF.

2. Materials and methods

2.1. Cell cultures

Mouse fibroblast L cells expressing mouse CL-1, CL-2, CL-3, CL-4, or CL-5 were kindly provided by Dr. S. Tsukita (Kyoto University). Cells were cultured in Eagle's minimum essential medium with 10% (v/v) fetal calf serum and 500 μg/ml G418 at 37 °C under a 5% (v/v) CO_2 atmosphere.

Please cite this article in press as: Li, X., et al. Tissue distribution and safety evaluation of a claudin-targeting molecule, the C-terminal fragment of *Clostridium perfringens* enterotoxin. Eur. J. Pharm. Sci. (2013), http://dx.doi.org/10.1016/j.ejps.2013.10.018

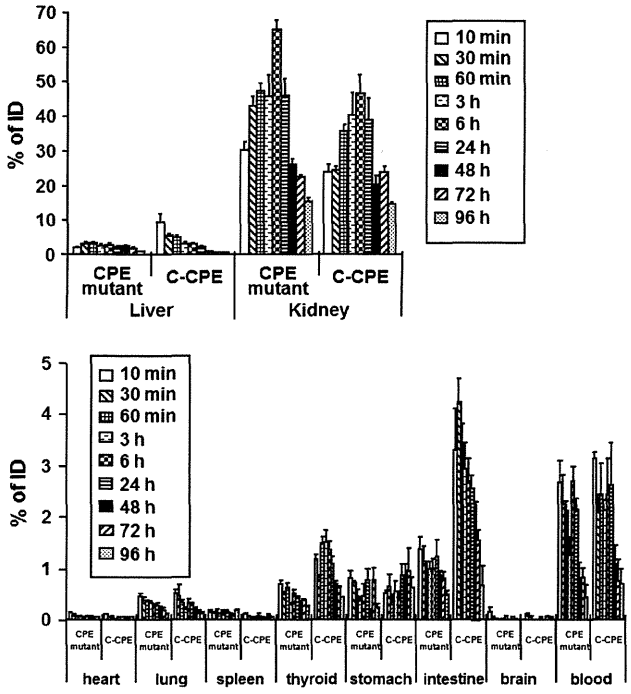

Fig. 2. *In vivo* distribution of the CF750-labeled C-terminal fragment of *Clostridium perfringens* enterotoxin (C-CPE). Mice were intravenously injected with 2 μg/mouse CF750-labeled C-CPE or a CF750-labeled C-CPE mutant. Tissues were removed at the indicated times after injection and the intensity of fluorescence of each tissue was measured as described in the Materials and Methods. Tissue C-CPE levels were calculated as percentages of injected doses. Data are means ± SEM (n = 5). ID, injected dose.

2.2. Preparation of C-CPE and C-CPE mutant protein

C-CPE, and a mutant form thereof, in which Ala was substituted with Tyr and Leu at positions 306 and 315, were prepared as described previously (Takahashi et al., 2008). Briefly, recombinant plasmids derived from pET-16b, pET-C-CPE encoding histidine (His)-tagged C-CPE, or a pET-C-CPE mutant encoding His-tagged C-CPE mutant protein, were transduced into *Escherichia coli* strain BL21 (DE3) (Novagen, Darmstadt, Germany), and production of recombinant proteins was induced by adding isopropyl-β-D-thiogalactopyranoside. Harvested cells were lysed in buffer A (10 mM Tris–HCl [pH 8.0], 400 mM NaCl, 5 mM $MgCl_2$, 0.1 mM phenylmethylsulfonyl fluoride, 1 mM 2-mercaptoethanol, and 10% [v/v] glycerol). Each lysate was applied to a HiTrap chelating HP column (GE Healthcare, Chalfont St Giles, Buckinghamshire, UK), and the recombinant protein was eluted with buffer A containing imidazole. This buffer was exchanged for phosphate-buffered saline (PBS) by using a PD-10 column (GE Healthcare), and the purified proteins dissolved in PBS were stored at −80 °C until use. The purity of the recombinant proteins was confirmed by sodium dodecyl sulfate–polyacrylamide gel electrophoresis followed by staining with Coomassie brilliant blue. Protein concentrations were quantified with a BCA protein assay kit, using bovine serum albumin (BSA) as a standard (Pierce Chemicals, Rockford, IL).

2.3. Animals

Female BALB/c mice (6–8 weeks of age) were purchased from SLC, Inc. (Shizuoka, Japan). Mice were housed at 23 ± 1.5 °C with a 12-h light/12-h dark cycle and had free access to water and commercial chow (Type MF; Oriental Yeast, Tokyo, Japan). Mice were allowed to adapt to these conditions for at least 1 week after arrival. All animal experiments adhered to the ethical guidelines of the Graduate School of Pharmaceutical Sciences, Osaka University.

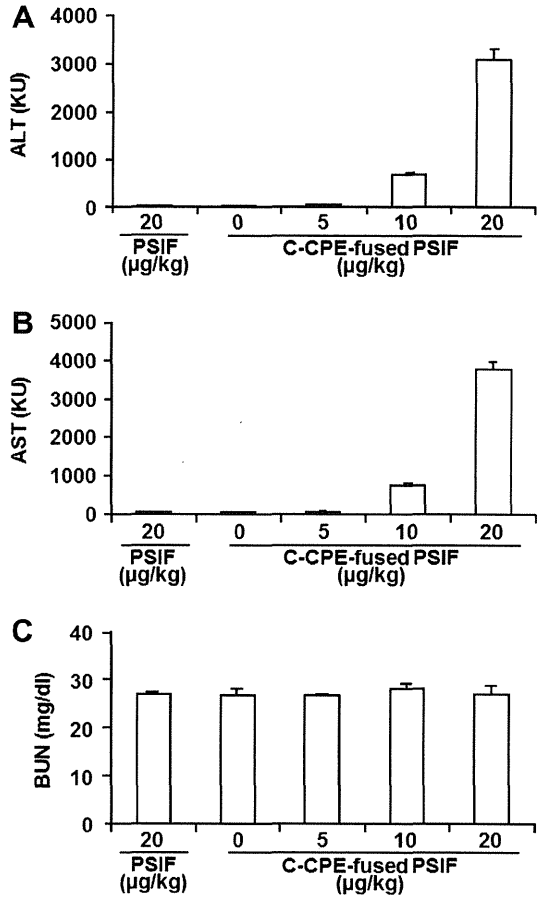

Fig. 3. Serum markers of liver and kidney injury in mice injected with protein synthesis inhibitory factor (PSIF) fused to the C-terminal fragment of *Clostridium perfringens* enterotoxin (C-CPE). Mice were intravenously injected with PSIF at 2 μg/kg or C-CPE-fused PSIF at 0, 5, 10, or 20 μg/kg. Twenty-four hours later, serum ALT (A), AST (B), and BUN (C) levels were measured as described in the Materials and Methods. Data are presented as means ± SEM (n = 5).

2.4. Preparation of CF750-labeled C-CPE proteins

C-CPE and the mutant form of the protein were labeled with the fluorescent dye CF750 by using a XenoLight CF750 rapid antibody-labeling kit (Caliper Life Sciences, Inc., Hopkinton, MA), in accordance with the manufacturer's instructions. The concentrations of labeled C-CPEs were calculated according to the manufacturer's protocol by using the following equation: Concentration (mg/ml) = {[absorbance at 280 nm minus (absorbance at 755 nm × 0.3)]/0.46} × dilution factor.

2.5. Fluorescence-activated cell sorter (FACS) analysis

L-cells expressing various CLs were harvested with trypsin and suspended in PBS. The cells were incubated with C-CPE or the mutant form of C-CPE for 1 h at 4 °C; this was followed by incubation with anti-His-tag antibody. Cells were next incubated with fluorescein-labeled secondary antibody, and cells that bound the test proteins were detected and analyzed by flow cytometry (FACScalibur, Becton Dickinson, Franklin Lakes, NJ).

2.6. Tissue distribution of injected proteins

C-CPE, or the mutant form thereof, labeled with CF750, was intravenously injected into mice at 2 μg/100 μl of PBS per mouse. Mice were sacrificed 10 min, 30 min, 60 min, 3 h, 6 h, 24 h, 48 h,

Please cite this article in press as: Li, X., et al. Tissue distribution and safety evaluation of a claudin-targeting molecule, the C-terminal fragment of *Clostridium perfringens* enterotoxin. Eur. J. Pharm. Sci. (2013), http://dx.doi.org/10.1016/j.ejps.2013.10.018

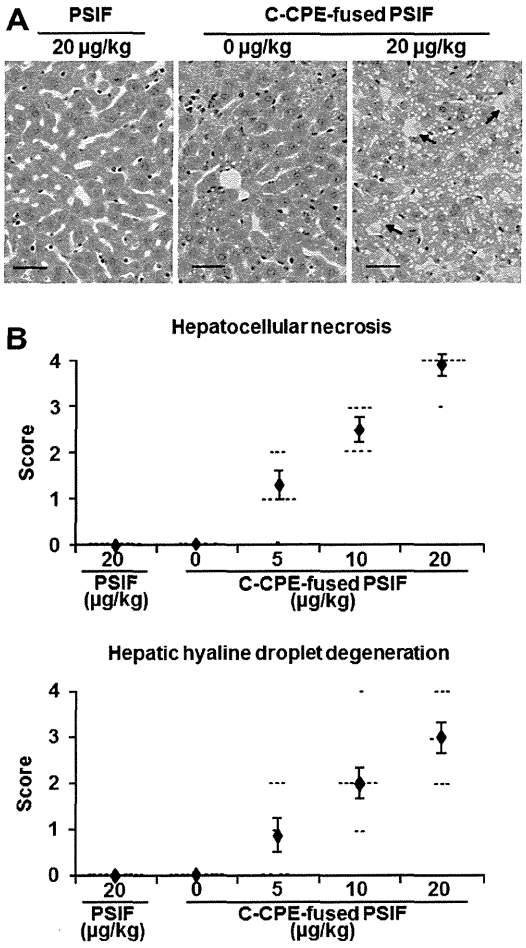

Fig. 4. Histological analysis of the livers of mice injected with protein synthesis inhibitory factor (PSIF) fused to the C-terminal fragment of *Clostridium perfringens* enterotoxin (C-CPE). Mice were intravenously injected with PSIF at 20 μg/kg or C-CPE-fused PSIF at 0, 5, 10, or 20 μg/kg ($n = 7$ or 8). Twenty-four hours later, the livers were removed and fixed in formaldehyde. Sections were stained with hematoxylin–eosin and examined microscopically for pathology. A representative micrograph is shown in panel A; arrows indicate regions of injury (scale bar, 60 μm). The extents of hepatocellular necrosis and hepatic hyaline droplet degeneration were scored (panel B) as follows: 0, none; 1, very mild; 2, mild; 3, moderate; or 4, high. Each horizontal dash represents the score of one sample. Data are means ± SEM ($n = 7$ or 8).

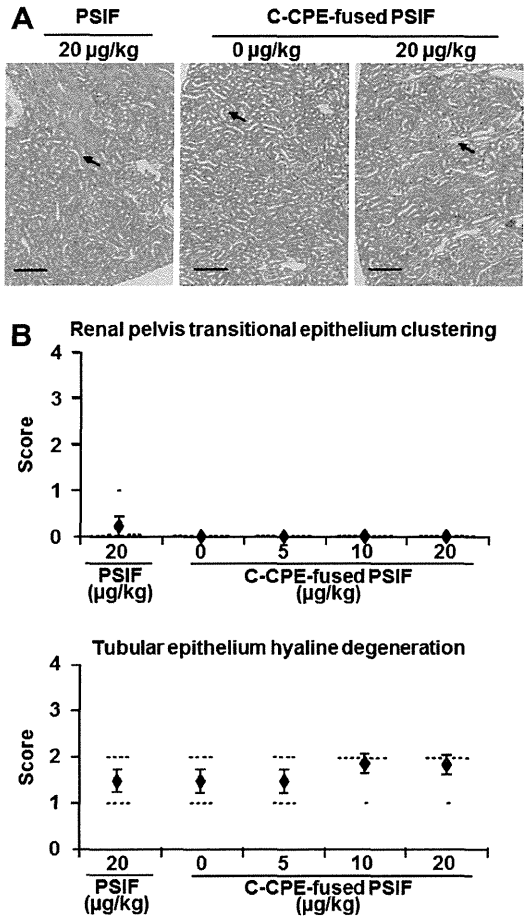

Fig. 5. Histological analysis of the kidneys of mice injected with protein synthesis inhibitory factor (PSIF) fused to the C-terminal fragment of *Clostridium perfringens* enterotoxin (C-CPE). Mice were intravenously injected with PSIF at 20 μg/kg or C-CPE-fused PSIF at 0, 5, 10, or 20 μg/kg ($n = 7$ or 8). Twenty-four hours later, the kidneys were removed and fixed in formaldehyde. Sections were stained with hematoxylin-eosin and examined microscopically for pathology. A representative micrograph is shown in panel A; arrows indicate regions of injury (scale bar, 240 μm). The extent of clustering of the renal pelvis transitional epithelium and the level of hyaline degeneration of the tubular epithelium were scored (panel B) as follows: 0, none; 1, very mild; 2, mild; 3, moderate; or 4, high. Each horizontal dash represents the score of one sample. Data are means ± SEM ($n = 7$ or 8).

72 h, or 96 h later. The blood, heart, lung, liver, spleen, kidney, thyroid, stomach, intestine, and brain were excised from each mouse. The blood and organs from each mouse were placed side-by-side and imaged by using a Maestro EX *in vivo* imaging system, version 2.10.0 (Cambridge Research & Instrumentation Inc., Woburn, MA). The imaging system was equipped with an excitation filter (wavelength 229–684 nm). Fluorescence was detected by a CCD camera equipped with a C-mount lens and a long-pass emission filter (745 nm). Spectral data "cubes" were created by acquisition of a series of images obtained by using different wavelengths. In such cubes, each pixel is associated with a spectrum. Maestro software can be used to analyze these data; any autofluorescence can be identified, separated from the CF750 fluorescence, and removed. The resulting signals (counts) from each tissue were used to evaluate C-CPE distributions. The levels of C-CPEs in each tissue, as percentages of injected doses, were calculated. Total blood volume was calculated as 8% of body weight.

2.7. Preparation of C-CPE-fused PSIF

PSIF and C-CPE-fused PSIF were prepared as described previously (Saeki et al., 2009). In brief, plasmid pET-PSIF or pET-C-CPE-PSIF was transduced into *E. coli* BL21 (DE3) and recombinant protein production was induced by adding 0.25 mM isopropyl-β-D-thiogalactopyranoside. Harvested cells were lysed in buffer A. The lysates were centrifuged and the supernatants applied to Hi-Trap chelating HP columns. Recombinant proteins were eluted with imidazole-containing buffer A. This buffer was exchanged for PBS by using a PD-10 column, and the purified protein solutions were stored at −80 °C until use. Protein concentrations were quantified with a BCA protein assay kit, using BSA as a standard.

2.8. Biochemical assays

Mice were intravenously injected with 100 μl of C-CPE-fused PSIF at 0, 5, 10, or 20 μg/kg, or with 100 μl of PSIF at 20 μg/kg.

Please cite this article in press as: Li, X., et al. Tissue distribution and safety evaluation of a claudin-targeting molecule, the C-terminal fragment of *Clostridium perfringens* enterotoxin. Eur. J. Pharm. Sci. (2013), http://dx.doi.org/10.1016/j.ejps.2013.10.018

Twenty-four hours after the injection, serum levels of alanine aminotransferase (ALT), aspartate aminotransferase (AST), and blood urea nitrogen (BUN) were measured with commercial kits (Transaminase-CII kit [ALT, AST] and Blood Urea Nitrogen-B Test [BUN]; Wako Pure Chemicals, Osaka, Japan).

2.9. Histological analysis

Livers and kidneys were removed and fixed in 4% (v/v) paraformaldehyde. Thin sections were stained with hematoxylin and eosin before histological observation. The extent of injury was scored as 0, none; 1, very mild; 2, mild; 3, moderate; or 4, high.

3. Results

3.1. Tissue distribution of the CL-3/-4-binding agent C-CPE

The fluorescent dye CF750 was conjugated to the CL-3/-4-binding agent C-CPE to allow the tissue distribution of C-CPE to be monitored. FACS analysis revealed that CF750-labeled C-CPE bound to CL-3- or CL-4-expressing L-cells but not to mock-, CL-1-, CL-2-, or CL-5-expressing L cells (Fig. 1). Thus, labeling of C-CPE with CF750 did not affect the binding profile of C-CPE to CLs. As a control, we also prepared a CF750-labeled C-CPE mutant protein lacking CL-binding activity; Ala was substituted for the wild-type Tyr306 and Leu315 in the mutant protein (Takahashi et al., 2008). The C-CPE mutant did not bind to the cells (Fig. 1).

C-CPE was evident in the kidney (24.0% of the injected dose), liver (9.5%), intestine (3.3%), and thyroid (1.2%) 10 min after intravenous injection (Fig. 2). The levels of C-CPE in the liver, intestine, and thyroid gradually fell thereafter, to 0.4%, 0.7%, and 0.4% of the injected dose, respectively, at 96 h post-injection. In contrast, the level of C-CPE in the kidney increased to 46.5% of the injected dose 6 h after injection and only then began to fall, reaching 14.4% of the injected dose 96 h post-injection. The control C-CPE mutant protein became distributed in the liver (2.0% of the injected dose), intestine (1.4%), and thyroid (0.7%) at levels much lower than those of C-CPE at 10 min post-injection, but the levels of the mutant protein in the kidney were comparable to those of C-CPE (Fig. 2). Therefore, the liver may be a major target tissue of CL-3/-4-binding protein, whereas accumulation in the kidney may not be associated with CL-3/-4 targeting.

3.2. Effects of a CL-3/-4-targeting toxin on the liver and kidney

We previously found that tail vein injection of C-CPE-fused PSIF at 5 μg/kg every 2 days for 14 days had anti-tumor activity without hepatotoxicity or nephrotoxicity (Saeki et al., 2010). Here, to evaluate the acute toxicity of a CL-targeting toxin to the liver and kidney, we intravenously injected mice with C-CPE-fused PSIF, or control PSIF alone, and measured biochemical markers of liver (ALT and AST) and kidney (BUN) injury 24-h later. Injection of PSIF alone (20 μg/kg) did not increase serum ALT, AST, or BUN levels. Injection of C-CPE-fused PSIF at doses of 0, 5, 10, and 20 μg/kg increased serum ALT and AST levels in a dose-dependent manner (ALT: 21, 49, 668, and 3053 karmen unit (KU) respectively; AST: 49, 68, 764, and 3781 KU, respectively) (Fig. 3A and B). In contrast, injection of C-CPE-fused PSIF, even at 20 μg/kg, did not increase the serum BUN level (Fig. 3C). Injection of C-CPE-fused PSIF at 10 or 20 μg/kg, but not at 5 μg/kg, caused body weight loss and reduced mobility (data not shown). Histologically, C-CPE-fused PSIF caused hepatocellular necrosis and hyaline droplet degeneration (Fig. 4A, B). Although injection of C-CPE-fused PSIF caused slight hyaline degeneration of the tubular epithelium of the kidney, injection of PSIF alone had a similar effect (Fig. 5A and B). Therefore, the low-level kidney injury evident after administration of C-CPE-fused PSIF may not have been associated with the targeting of CLs.

4. Discussion

CPE was the first CL-3/-4-targeting toxin to be described (Fujita et al., 2000; Sonoda et al., 1999), and C-CPE-fused PSIF was the second (Ebihara et al., 2006; Saeki et al., 2009). A series of studies using CPE and C-CPE have provided proof-of-concept that CL targeting is a strategy for cancer therapy (Long et al., 2001; Michl et al., 2001; Neesse et al., 2013; Saeki et al., 2009, 2010; Santin et al., 2005). However, because CL-3 and CL-4 are expressed in various normal tissues (Morita et al., 1999; Turksen and Troy, 2011), risk assessment of CL-targeting molecules is needed when CPE technology is applied to cancer therapy. Here, we found that systemic injection of a C-CPE-fused toxin resulted in acute hepatic, but not renal, toxicity 24 h after injection in mice.

After injection, C-CPE accumulates to the greatest extent in the liver and kidney. The expression profiles of CL-3 and CL-4 differ in these two tissues. In the liver, CL-3 is locally expressed in the lateral membranes of all lobular hepatocytes (Rahner et al., 2001); the liver does not express CL-4 (Morita et al., 1999). In contrast, CL-3 and CL-4 are locally expressed, in the kidney, in the lateral membranes of epithelial-cell sheets of the loop of Henle, the distal tubule, and the collecting duct (Balkovetz, 2009). Epithelial cells of the kidney form a boundary between the inner and outer regions, and the TJs act as barriers, preventing free movement of solutes across epithelial sheets (Hou et al., 2010; Milatz et al., 2010). In contrast, hepatocytes do not have a barrier function, with the exception of those located in the canaliculi. Therefore, CL-targeting molecules can access CL-3 in parts of the liver other than the canaliculi, but not CL-3 and CL-4 in the renal epithelium. C-CPE-fused PSIF must be taken up by cells if the drug is to be cytotoxic, because inhibition of ribosomal elongation factor-2 by the PSIF domain is the cause of cell death (Ebihara et al., 2006; Kreitman and Pastan, 2006; Ogata et al., 1990).

Here, we found that hepatic accumulation of a toxin fused to C-CPE could have adverse effects if C-CPE-based cancer therapy were prescribed. C-CPE binds to both CL-3 and CL-4. Levels of CL-4 are increased more frequently than those of CL-3 in cancers such as breast, gastric, intestinal, ovarian, pancreatic, and prostate carcinomas (Singh et al., 2010; Tsukita et al., 2008; Turksen and Troy, 2011). Thus, development of a C-CPE mutant that binds to CL-4 but not to CL-3 may be useful in cancer therapy. We previously found that modulation of the electrostatic profile of the C-CPE surface can change the CL-binding profile (Takahashi et al., 2012). Veshnyakova et al. (2012) showed that the C-CPE residues, Leu223, Asp225, and Arg227, were involved in binding to CL-3, whereas Leu254, Ser256, Ile258, and Asp284 were involved in binding to CL-4. Manipulation of the electrostatic surface and the C-CPE residues may allow us to develop a C-CPE mutant that binds specifically to CL-4.

Acknowledgements

We thank the staff of our laboratory for their useful comments and discussion. This work was supported by Grants-in-Aids for Scientific Research from the Ministry of Education, Culture, Sports, Science, and Technology of Japan (Nos. 21689006 and 24390042); by a Health and Labor Sciences Research Grant from the Ministry of Health, Labour, and Welfare of Japan; by the Takeda Science Foundation; by the Nakatomi Foundation; and by the Platform for Drug Discovery, Informatics, and Structural Life Science of the Ministry of Education, Culture, Sports, Science, and Technology, Japan.

Please cite this article in press as: Li, X., et al. Tissue distribution and safety evaluation of a claudin-targeting molecule, the C-terminal fragment of *Clostridium perfringens* enterotoxin. Eur. J. Pharm. Sci. (2013), http://dx.doi.org/10.1016/j.ejps.2013.10.018

References

Adair, J.R., Howard, P.W., Hartley, J.A., Williams, D.G., Chester, K.A., 2012. Antibody-drug conjugates – a perfect synergy. Expert. Opin. Biol. Ther. 12, 1191–1206.

Anderson, J.M., Van Itallie, C.M., 2009. Physiology and function of the tight junction. Cold Spring Harbor Perspect. Biol. 1, a002584.

Balkovetz, D.F., 2009. Tight junction claudins and the kidney in sickness and in health. Biochim. Biophys. Acta 1788, 858–863.

Dent, S., Oyan, B., Honig, A., Mano, M., Howell, S., 2013. HER2-targeted therapy in breast cancer: a systematic review of neoadjuvant trials. Cancer Treat. Rev. 39, 622–631.

Ebihara, C., Kondoh, M., Hasuike, N., Harada, M., Mizuguchi, H., Horiguchi, Y., Fujii, M., Watanabe, Y., 2006. Preparation of a claudin-targeting molecule using a C-terminal fragment of *Clostridium perfringens* enterotoxin. J. Pharmacol. Exp. Ther. 316, 255–260.

Farquhar, M.G., Palade, G.E., 1963. Junctional complexes in various epithelia. J. Cell Biol. 17, 375–412.

Fujita, K., Katahira, J., Horiguchi, Y., Sonoda, N., Furuse, M., Tsukita, S., 2000. *Clostridium perfringens* enterotoxin binds to the second extracellular loop of claudin-3, a tight junction integral membrane protein. FEBS Lett. 476, 258–261.

Furuse, M., Tsukita, S., 2006. Claudins in occluding junctions of humans and flies. Trends Cell Biol. 16, 181–188.

Hou, J., Renigunta, A., Yang, J., Waldegger, S., 2010. Claudin-4 forms paracellular chloride channel in the kidney and requires claudin-8 for tight junction localization. Proc. Natl. Acad. Sci. USA 107, 18010–18015.

Jemal, A., Siegel, R., Ward, E., Hao, Y., Xu, J., Murray, T., Thun, M.J., 2008. Cancer statistics, 2008. CA Cancer J. Clin. 58, 71–96.

Kreitman, R.J., Pastan, I., 2006. Immunotoxins in the treatment of hematologic malignancies. Curr. Drug Targets 7, 1301–1311.

Long, H., Crean, C.D., Lee, W.H., Cummings, O.W., Gabig, T.G., 2001. Expression of *Clostridium perfringens* enterotoxin receptors claudin-3 and claudin-4 in prostate cancer epithelium. Cancer Res. 61, 7878–7881.

McClane, B.A., Chakrabarti, G., 2004. New insights into the cytotoxic mechanisms of *Clostridium perfringens* enterotoxin. Anaerobe 10, 107–114.

Michl, P., Buchholz, M., Rolke, M., Kunsch, S., Lohr, M., McClane, B., Tsukita, S., Leder, G., Adler, G., Gress, T.M., 2001. Claudin-4: a new target for pancreatic cancer treatment using *Clostridium perfringens* enterotoxin. Gastroenterology 121, 678–684.

Milatz, S., Krug, S.M., Rosenthal, R., Gunzel, D., Muller, D., Schulzke, J.D., Amasheh, S., Fromm, M., 2010. Claudin-3 acts as a sealing component of the tight junction for ions of either charge and uncharged solutes. Biochim. Biophys. Acta 1798, 2048–2057.

Mineta, K., Yamamoto, Y., Yamazaki, Y., Tanaka, H., Tada, Y., Saito, K., Tamura, A., Igarashi, M., Endo, T., Takeuchi, K., Tsukita, S., 2011. Predicted expansion of the claudin multigene family. FEBS Lett. 585, 606–612.

Morita, K., Furuse, M., Fujimoto, K., Tsukita, S., 1999. Claudin multigene family encoding four-transmembrane domain protein components of tight junction strands. Proc. Natl. Acad. Sci. USA 96, 511–516.

Neesse, A., Hahnenkamp, A., Griesmann, H., Buchholz, M., Hahn, S.A., Maghnouj, A., Fendrich, V., Ring, J., Sipos, B., Tuveson, D.A., Bremer, C., Gress, T.M., Michl, P., 2013. Claudin-4-targeted optical imaging detects pancreatic cancer and its precursor lesions. Gut 62, 1034–1043.

Ogata, M., Chaudhary, V.K., Pastan, I., FitzGerald, D.J., 1990. Processing of *Pseudomonas* exotoxin by a cellular protease results in the generation of a 37,000-Da toxin fragment that is translocated to the cytosol. J. Biol. Chem. 265, 20678–20685.

Rahner, C., Mitic, L.L., Anderson, J.M., 2001. Heterogeneity in expression and subcellular localization of claudins 2, 3, 4, and 5 in the rat liver, pancreas, and gut. Gastroenterology 120, 411–422.

Rodriguez-Boulan, E., Nelson, W.J., 1989. Morphogenesis of the polarized epithelial cell phenotype. Science 245, 718–725.

Saeki, R., Kondoh, M., Kakutani, H., Tsunoda, S., Mochizuki, Y., Hamakubo, T., Tsutsumi, Y., Horiguchi, Y., Yagi, K., 2009. A novel tumor-targeted therapy using a claudin-4-targeting molecule. Mol. Pharmacol. 76, 918–926.

Saeki, R., Kondoh, M., Kakutani, H., Matsuhisa, K., Takahashi, A., Suzuki, H., Kakamu, Y., Watari, A., Yagi, K., 2010. A claudin-targeting molecule as an inhibitor of tumor metastasis. J. Pharmacol. Exp. Ther. 334, 576–582.

Santin, A.D., Cane, S., Bellone, S., Palmieri, M., Siegel, E.R., Thomas, M., Roman, J.J., Burnett, A., Cannon, M.J., Pecorelli, S., 2005. Treatment of chemotherapy-resistant human ovarian cancer xenografts in C.B-17/SCID mice by intraperitoneal administration of *Clostridium perfringens* enterotoxin. Cancer Res. 65, 4334–4342.

Singh, A.B., Sharma, A., Dhawan, P., 2010. Claudin family of proteins and cancer: an overview. J. Oncol. 2010, 541957.

Sonoda, N., Furuse, M., Sasaki, H., Yonemura, S., Katahira, J., Horiguchi, Y., Tsukita, S., 1999. *Clostridium perfringens* enterotoxin fragment removes specific claudins from tight junction strands: evidence for direct involvement of claudins in tight junction barrier. J. Cell Biol. 147, 195–204.

Staehelin, L.A., 1973. Further observations on the fine structure of freeze-cleaved tight junctions. J. Cell Sci. 13, 763–786.

Takahashi, A., Komiya, E., Kakutani, H., Yoshida, T., Fujii, M., Horiguchi, Y., Mizuguchi, H., Tsutsumi, Y., Tsunoda, S., Koizumi, N., Isoda, K., Yagi, K., Watanabe, Y., Kondoh, M., 2008. Domain mapping of a claudin-4 modulator, the C-terminal region of C-terminal fragment of *Clostridium perfringens* enterotoxin, by site-directed mutagenesis. Biochem. Pharmacol. 75, 1639–1648.

Takahashi, A., Saito, Y., Kondoh, M., Matsushita, K., Krug, S.M., Suzuki, H., Tsujino, H., Li, X., Aoyama, H., Matsuhisa, K., Uno, T., Fromm, M., Hamakubo, T., Yagi, K., 2012. Creation and biochemical analysis of a broad-specific claudin binder. Biomaterials 33, 3464–3474.

Tsukita, S., Yamazaki, Y., Katsuno, T., Tamura, A., Tsukita, S., 2008. Tight junction-based epithelial microenvironment and cell proliferation. Oncogene 27, 6930–6938.

Turksen, K., Troy, T.C., 2011. Junctions gone bad: claudins and loss of the barrier in cancer. Biochim. Biophys. Acta 1816, 73–79.

Vermeer, P.D., Einwalter, L.A., Moninger, T.O., Rokhlina, T., Kern, J.A., Zabner, J., Welsh, M.J., 2003. Segregation of receptor and ligand regulates activation of epithelial growth factor receptor. Nature 422, 322–326.

Veshnyakova, A., Piontek, J., Protze, J., Waziri, N., Heise, I., Krause, G., 2012. Mechanism of *Clostridium perfringens* enterotoxin interaction with claudin-3/-4 protein suggests structural modifications of the toxin to target specific claudins. J. Biol. Chem. 287, 1698–1708.

Wodarz, A., Nathke, I., 2007. Cell polarity in development and cancer. Nat. Cell Biol. 9, 1016–1024.

Yewale, C., Baradia, D., Vhora, I., Misra, A., 2013. Proteins: emerging carrier for delivery of cancer therapeutics. Expert Opin. Drug Deliv. 10, 1429–1448.

Zouhairi, M., Charabaty, A., Pishvaian, M.J., 2011. Molecularly targeted therapy for metastatic colon cancer: proven treatments and promising new agents. Gastrointest. Cancer Res. 4, 15–21.

Please cite this article in press as: Li, X., et al. Tissue distribution and safety evaluation of a claudin-targeting molecule, the C-terminal fragment of *Clostridium perfringens* enterotoxin. Eur. J. Pharm. Sci. (2013), http://dx.doi.org/10.1016/j.ejps.2013.10.018

A Baculoviral Display System to Assay Viral Entry

Manami Iida,[a,#] Takeshi Yoshida,[a,#] Akihiro Watari,[a] Kiyohito Yagi,[a] Takao Hamakubo,[b] and Masuo Kondoh*,[a]

[a] *Laboratory of Bio-Functional Molecular Chemistry, Graduate School of Pharmaceutical Sciences, Osaka University; Suita, Osaka 565–0871, Japan: and* [b] *Department of Quantitative Biology and Medicine, Research Center for Advanced Science and Technology, The University of Tokyo; Tokyo 153–8904, Japan.*
Received August 9, 2013; accepted August 22, 2013

In this study, we evaluated a baculoviral display system for analysis of viral entry by using a recombinant adenovirus (Ad) carrying a luciferase gene and budded baculovirus (BV) that displays the adenoviral receptor, coxsackievirus and adenovirus receptor (CAR). CAR-expressing B16 cells (B16-CAR cells) were infected with luciferase-expressing Ad vector in the presence of BV that expressed or lacked CAR (CAR-BV and mock-BV, respectively). Treatment with mock-BV even at doses as high as 5 μg/mL failed to attenuate the luciferase activity of B16-CAR cells. In contrast, treatment with CAR-BV with doses as low as 0.5 μg/mL significantly decreased the luciferase activity of infected cells, which reached 65% reduction at 5 μg/mL. These findings suggest that a receptor-displaying BV system could be used to evaluate viral infection.

Key words baculovirus; virus; infection; receptor

The process of viral infection involves entry of the virus into the cell, followed by replication of the viral genome and other viral components in the host cell.[1] Whereas the molecular mechanisms underlying viral replication have largely been elucidated, the key molecules for entry, the viral receptors on host cells, have never been fully identified. Most host receptors are integral membrane proteins, and it is difficult to prepare their recombinant proteins because of their hydrophobicity. Since recombinant proteins are needed to screen inhibitors for viral entry and to produce antibodies against host receptors, preparation of inhibitors, such as chemicals, peptides and antibodies, for viral entry has been delayed.

The baculoviral expression system in insect cells has been widely used for preparation of recombinant proteins.[2] Hamakubo and colleagues found that baculoviral particles are released from baculovirus-infected cells; the membranes of these budded baculovirus (BV) display host-cell-derived membrane proteins.[3] Interestingly, the activity and topology of these host-origin proteins remain intact in the baculoviral membrane.[4] Moreover, a baculoviral envelope protein gp64 trasngenic mice were generated, and method to generate monoclonal antibodies against membrane proteins by immunization of gp64 transgenic mice with membrane protein-displayed baculovirus has been established.[5] These findings suggest that a baculoviral display system may be useful for assaying viral entry, leading to creation of monoclonal antibodies against host receptors.

In the present study, we investigated whether a baculoviral display system work as an assay system for viral entry using recombinant adenovirus (Ad) vector and a receptor for Ad, coxsackievirus and adenovirus receptor (CAR).[6]

MATERIALS AND METHODS

Cell Culture Mouse melanoma B16-CAR cells[7] were cultured in Dulbecco's modified Eagle's medium (DMEM) supplemented with 10% fetal calf serum (FCS) and 2 mg/mL G418. 293 cells were cultured in DMEM supplemented with 10% FCS. Sf9 cells (Invitrogen, Gaithersburg, MD, U.S.A.) were cultured in Grace's insect cell culture medium supplemented with 10% FCS.

Preparation of Recombinant Ad Vector An improved *in vitro* ligation method[8] was used to generate a recombinant type 5 Ad vector that encoded a fusion protein comprising enhanced green fluorescence protein and firefly luciferase (EGFPLuc). The recombinant Ad vector (Ad-EGFPLuc) was purified from transfected cells by using $CsCl_2$ gradient centrifugation. Viral titers were determined spectrophotometrically.[9]

Preparation of Recombinant Baculoviruses Recombinant BVs were prepared by using the Bac-to-Bac Baculovirus Expression System (Invitrogen) according to the manufacturer's protocol. Sf9 cells were transduced with the CAR-encoding bacmid, recombinant CAR-BV were recovered by centrifugation of the conditioned medium,[10] and Sf9 cells were infected with recombinant CAR-BV. At 72 h after infection, the culture supernatant of the infected Sf9 cells was centrifuged to pellet recombinant CAR-BV, which were resuspended in Tris-buffered saline and stored at 4°C until use.

Western Blotting Mock-BV, CAR-BV, and B16-CAR cells were lysed in lysis buffer (25 mM Tris–HCl [pH 7.5], 1% Triton X-100, 0.5% sodium deoxycholate, 150 mM NaCl, 5 mM ethylenediaminetetraacetic acid (EDTA)) containing protease inhibitors (Sigma, St. Louis, MO, U.S.A.). The protein content of the resulting lysates was measured by using the BCA protein assay kit (Pierce Chemical, Rockford, IL, U.S.A.), with bovine serum albumin as the standard. Samples of cellular lysates (20 μg) and BV lysates (5 μg) underwent sodium dodecyl sulfate–polyacrylamide gel electrophoresis followed by blotting of proteins to a polyvinylidene difluoride membrane. The membrane was treated with 5% skim milk to inhibit nonspecific binding, incubated with an anti-goat CAR antibody (R&D Systems, Minneapolis, MN, U.S.A.), and then incubated with a peroxidase-labeled secondary antibody. Immunoreactive bands were visualized by using chemiluminescence reagents (GE Healthcare, Buckinghamshire, U.K.).

Infection Assay Aliquots of Ad-EGFPLuc vector (4×10^7

The authors declare no conflict of interest.

[#] These authors contributed equally to this work.

* To whom correspondence should be addressed. e-mail: masuo@phs.osaka-u.ac.jp

viral particles per mL) were incubated with mock-BV or CAR-BV (0.5 or 5 μg/mL) and an anti-BV gp64 antibody (0.065 or 0.65 μg/mL; AcV1, Santa Cruz Biotechnology, CA, U.S.A.) for 2 h at 37°C to prevent non-specific binding of gp64 to cells. B16-CAR cells were seeded onto 96-well plates (2×10^4 cells per well); 50 μL of the mixture of Ad vector and BVs was added to each well and incubated for 15 min, after which the medium was replaced with fresh growth medium. After an additional 24 h of culture, the luciferase activity in the lysates was measured by using a luminometer.

Statistical Analysis The data were analyzed for statistical significance by Student's *t*-test.

RESULTS AND DISCUSSION

First, we prepared CAR-displaying BV. Lysates of CAR-B16 cells, a mouse myeloma line that expresses mouse CAR, yielded two bands, at 40 and 46 kDa (Fig. 1). In contrast, lysates of CAR-BV showed not only the 40-kDa form but also several bands lower and upper than 40 kDa (Fig. 1); these bands likely represent post-translational modifications. CAR contains two *N*-glycosylation sites and two disulfide-bonded loops in the extracellular domain. The putative molecular sizes of CAR are 40 and 46 kDa, in its non-glycosylated form and glycosylated forms, respectively.[6] Protein folding and post-translational processing, particularly *N*-glycosylation, in insect cells differs markedly from that in mammal cells.[11–13] For example, prolactin receptor expressed in insect cells was 29 kDa larger than that expressed in mammalian cells; this difference was attributed to *N*-glycosylation and ubiquitination.[14]

To investigate whether CAR-BV inhibited adenoviral entry, B16-CAR cells were infected with Ad vector expressing luciferase in the presence of mock-BV or CAR-BV. Whereas treatment with mock-BV at doses as high as 5 μg/mL did not attenuate the luciferase activity of the infected B16-CAR cells, treatment with as little as 0.5 μg/mL CAR-BV significantly decreased their luciferase activity, which reaching 65% reduction at 5 μg/mL (Fig. 2). These findings indicate that CAR-BV prevented the infection of cells by Ad vector. In support of our finding, recombinant prolactin receptor expressed in insect cells and prolactin receptor purified from rabbit mammary gland showed similar specificity and affinity to prolactin.[14] Accordingly, the post-translational modification of CAR in insect cells may not hamper the ability of Ad vector to bind to its receptor.

Our current findings suggest that a baculoviral display system may be useful in the analysis of viral infection, which involves binding of the viral envelope to the viral receptor in the membrane of the host cell. Baculoviral display systems have also been used widely to generate monoclonal antibodies against the extracellular regions of membrane proteins.[3,15] Future applications of baculoviral display systems might contribute the analysis of the mechanisms underlying the entry of pathogens into host cells and the generation of inhibitors of viral entry.

Acknowledgments We thank Prof. H. Mizuguchi (Osaka University) and the members of our laboratory for providing us CAR cDNA and CAR-expressing B16 cells, and useful comments, respectively. This work was supported by a Grant-in-Aid for Scientific Research from the Ministry of Education, Culture, Sports, Science and Technology of Japan (24390042), by a Health and Labour Sciences Research Grant from the Ministry of Health, Labor, and Welfare of Japan, the Takeda Science Foundation and the Nakatomi Foundation.

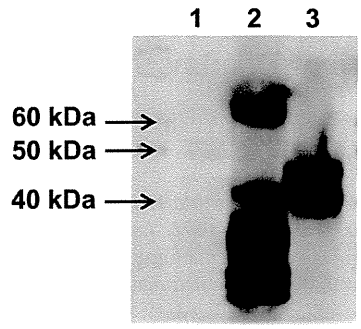

Fig. 1. Preparation of CAR-Displaying BV

Lysates of mock-BV (5 μg, lane 1), CAR-BV (5 μg, lane 2), and CAR-B16 cells (20 μg, lane 3) underwent Western blotting by using a polyclonal goat anti-CAR antibody and a peroxidase-labeled secondary antibody. The arrows indicate the positions of marker proteins.

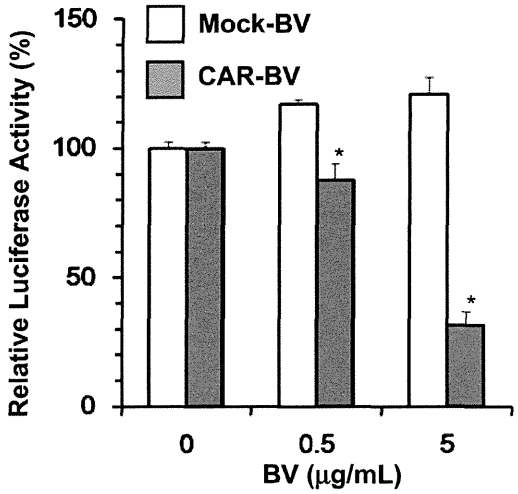

Fig. 2. Effects of CAR-Displaying BV on Ad Vector Infection

Ad vectors (4×10^7 viral particles per mL) were incubated with mock-BV or CAR-BV at 0, 0.5, or 5 μg/mL for 2 h at 37°C. B16-CAR cells were exposed to the Ad–BV mixtures, cultured for 24 h in fresh medium, lysed, and evaluated for luciferase activity. Data are given as luciferase activity relative to that of cells not exposed to BV. Data are shown as mean±S.D. (n=3). *Significant difference compared with mock-BV ($p<0.05$).

REFERENCES

1) Cosset FL, Lavillette D. Cell entry of enveloped viruses. *Adv. Genet.*, **73**, 121–183 (2011).
2) Bieniossek C, Imasaki T, Takagi Y, Berger I. MultiBac: expanding the research toolbox for multiprotein complexes. *Trends Biochem. Sci.*, **37**, 49–57 (2012).
3) Tanaka T, Takeno T, Watanabe Y, Uchiyama Y, Murakami T, Yamashita H, Suzuki A, Aoi R, Iwanari H, Jiang SY, Naito M, Tachibana K, Doi T, Shulman AI, Mangelsdorf DJ, Reiter R, Auwerx J, Hamakubo T, Kodama T. The generation of monoclonal antibodies against human peroxisome proliferator-activated receptors (PPARs). *J. Atheroscler. Thromb.*, **9**, 233–242 (2002).
4) Sakihama T, Masuda K, Sato T, Doi T, Kodama T, Hamakubo T. Functional reconstitution of G-protein-coupled receptor-mediated adenylyl cyclase activation by a baculoviral co-display system. *J.*

Biotechnol., **135**, 28–33 (2008).
5) Saitoh R, Ohtomo T, Yamada Y, Kodama N, Nezu J, Kimura N, Funahashi S, Furugaki K, Yoshino T, Kawase Y, Kato A, Ueda O, Jishage K, Suzuki M, Fukuda R, Arai M, Iwanari H, Takahashi K, Sakihama T, Ohizumi I, Kodama T, Tsuchiya M, Hamakubo T. Viral envelope protein gp64 transgenic mouse facilitates the generation of monoclonal antibodies against exogenous membrane proteins displayed on baculovirus. *J. Immunol. Methods*, **322**, 104–117 (2007).
6) Arnberg N. Adenovirus receptors: implications for targeting of viral vectors. *Trends Pharmacol. Sci.*, **33**, 442–448 (2012).
7) Yamashita M, Ino A, Kawabata K, Sakurai F, Mizuguchi H. Expression of coxsackie and adenovirus receptor reduces the lung metastatic potential of murine tumor cells. *Int. J. Cancer*, **121**, 1690–1696 (2007).
8) Mizuguchi H, Kay MA. A simple method for constructing E1- and E1/E4-deleted recombinant adenoviral vectors. *Hum. Gene Ther.*, **10**, 2013–2017 (1999).
9) Maizel JV Jr, White DO, Scharff MD. The polypeptides of adenovirus. I. Evidence for multiple protein components in the virion and a comparison of types 2, 7A, and 12. *Virology*, **36**, 115–125 (1968).
10) Saeki R, Kondoh M, Kakutani H, Tsunoda S, Mochizuki Y, Hamakubo T, Tsutsumi Y, Horiguchi Y, Yagi K. A novel tumor-targeted therapy using a claudin-4-targeting molecule. *Mol. Pharmacol.*, **76**, 918–926 (2009).
11) Altmann F, Staudacher E, Wilson IB, Marz L. Insect cells as hosts for the expression of recombinant glycoproteins. *Glycoconj. J.*, **16**, 109–123 (1999).
12) Voss T, Ergulen E, Ahorn H, Kubelka V, Sugiyama K, Maurer-Fogy I, Glossl J. Expression of human interferon omega 1 in Sf9 cells. No evidence for complex-type *N*-linked glycosylation or sialylation. *Eur. J. Biochem.*, **217**, 913–919 (1993).
13) Yeh JC, Seals JR, Murphy CI, van Halbeek H, Cummings RD. Site-specific *N*-glycosylation and oligosaccharide structures of recombinant HIV-1 gp120 derived from a baculovirus expression system. *Biochemistry*, **32**, 11087–11099 (1993).
14) Cahoreau C, Petridou B, Cerutti M, Djiane J, Devauchelle G. Expression of the full-length rabbit prolactin receptor and its specific domains in baculovirus infected insect cells. *Biochimie*, **74**, 1053–1065 (1992).
15) Hayashi I, Takatori S, Urano Y, Miyake Y, Takagi J, Sakata-Yanagimoto M, Iwanari H, Osawa S, Morohashi Y, Li T, Wong PC, Chiba S, Kodama T, Hamakubo T, Tomita T, Iwatsubo T. Neutralization of the gamma-secretase activity by monoclonal antibody against extracellular domain of nicastrin. *Oncogene*, **31**, 787–798 (2012).

Journal of
PERIODONTAL RESEARCH

J Periodont Res 2013

JOURNAL OF PERIODONTAL RESEARCH
doi:10.1111/jre.12119

Gene delivery to periodontal tissue using Bubble liposomes and ultrasound

M. Sugano[1,2], Y. Negishi[2], Y. Endo-Takahashi[2], N. Hamano[2], M. Usui[3], R. Suzuki[4], K. Maruyama[4], Y. Aramaki[2], M. Yamamoto[1]

[1]Department of Periodontology, Showa University School of Dentistry, Tokyo, Japan, [2]Department of Drug Delivery and Molecular Biopharmaceutics, School of Pharmacy, Tokyo University of Pharmacy and Life Sciences, Tokyo, Japan, [3]Division of Periodontology, Kyushu Dental University, Kokurakita-ku, Kitakyushu City, Japan and [4]Laboratory of Drug and Gene Delivery, Faculty of Pharma-Sciences, Teikyo University, Tokyo,Japan

Sugano M, Negishi Y, Endo-Takahashi Y, Hamano N, Usui M, Suzuki R, Maruyama K, Aramaki Y, Yamamoto M. Gene delivery to periodontal tissue using Bubble liposomes and ultrasound. J Periodont Res 2013; doi: 10.1111/jre.12119. © 2013 John Wiley & Sons A/S. Published by John Wiley & Sons Ltd

Background and Objective: Periodontitis is the most common inflammatory disease caused by oral biofilm infection. For efficient periodontal treatment, it is important to enhance the outcome of existing regenerative therapies. The physical action of an ultrasound may be able to deliver a therapeutic gene or drugs into the local area of the periodontium being treated for periodontal regeneration. Previously, we developed "Bubble liposomes" as a useful carrier for gene or drug delivery, and reported that delivery efficiency was increased with high-frequency ultrasound *in vitro* and *in vivo*. Hence, the aim of the present study was to examine the possibility of delivering genes into gingival tissues using Bubble liposomes and ultrasound.

Material and Methods: We attempted to deliver naked plasmid DNA encoding luciferase or enhanced green fluorescent protein (EGFP) into the lower labial gingiva of Wistar rats using Bubble liposomes, with or without ultrasound exposure. Ultrasound parameters were optimized for intensity (0-4.0 W/cm^2) and exposure time (0–120 s) to establish the most efficient conditions for exposure. The efficacy and duration of gene expression in the gingiva were investigated using a luciferase assay and fluorescence microscopy.

Results: The strongest relative luciferase activity was observed when rats were treated under the following ultrasound conditions: 2.0 W/cm^2 intensity and 30 s of exposure time. Relative luciferase activity, 1 d after gene delivery, was significantly higher in gingiva treated using Bubble liposomes and ultrasound than in gingiva of the other treatment groups. Histological analysis also showed that distinct EGFP-expressing cells were observed in transfected gingiva when rats were treated under optimized conditions.

Conclusion: From these results, the combination of Bubble liposomes and ultrasound provides an efficient technique for delivering plasmid DNA into the gingiva. This technique can be applied for the delivery of a variety of therapeutic molecules into target tissue, and may serve as a useful treatment strategy for periodontitis.

Yoichi Negishi, PhD, Department of Drug Delivery and Molecular Biopharmaceutics, School of Pharmacy, Tokyo University of Pharmacy and Life Sciences 1432-1 Horinouchi, Hachioji, Tokyo 192-0392 Japan
Tel: +81 42 676 3183
Fax: +81 42 676 3182
e-mail: negishi@toyaku.ac.jp

Key words: Bubble liposomes; gene delivery; periodontitis; ultrasound

Accepted for publication June 06, 2013

Periodontitis is the most common oral inflammatory disease. The pathogenic factor is a biofilm, also called dental plaque, which is composed of periodontal bacteria. Dental biofilms, particularly in deep periodontal pockets, cause inflammatory destruction of periodontal tissues, resulting in alveolar bone absorption and tooth loss. Two main strategies for periodontal therapy exist: infection control and periodontal regeneration. Periodontitis

is regarded as a local infection because it is an inflammatory disease mainly caused by dental biofilms. Therefore, the majority of conventional treatments aim to remove the biofilm on the local periodontium. For example, a local drug-delivery system is positioned as an adjunctive therapy in nonsurgical periodontal management, and some antibiotics have been orally administered to combat bacteria located in periodontal pockets. In order to maintain an effective concentration of tetracycline, the controlled release of tetracycline paste into the deep pockets of patients with periodontitis has been reported (1). However, an efficient periodontal antibiotic-delivery system that exhibits clinical therapeutic effectiveness has yet to be established.

On the other hand, periodontal regenerative therapy is regarded as an effective method of stimulating and guiding proliferating periodontal stem cells in the surrounding periodontal tissue. A large number of clinical studies have shown significant bone fill or clinical attachment level gain when an enamel matrix derivative, guided tissue-regeneration membranes and/or bone grafts were used for treatment of bone defects (2,3). However, there are also limitations in the indication of periodontal regenerative therapy and it is difficult to regenerate lost periodontal tissues. The development of more efficient periodontal therapy based on a new concept is needed, and an absolute treatment strategy may be established by utilizing a method that promotes the effects of existing treatments.

The latest developments reported have shown that gene delivery has the potential to promote wound healing or reduce healing complications that prevent regeneration (4,5). If wound healing in the local periodontium can be promoted during periodontal regeneration, it may lead to rapid recovery. Gene delivery into periodontal tissues may contribute to the up-regulation of neovascularization and cell proliferation, which are important factors for sufficient regeneration. However, technical limitations in *in-vivo* studies, including release control, stability, safety and/or convenience, still need to be overcome. Recently, the use of ultrasound (US), as physical energy to enhance the permeability of mucosa or skin, has been reported (6,7). In addition, the effects of US can be applied to enhance the delivery of therapeutic molecules, such as genes, drugs or peptides, into target tissues. The mechanism of gene delivery with US exposure is "cavitation", which generates many microbubbles and then results in their destruction. The efficiency of cavitation is enhanced by combining US with synthetic microbubbles such as Optison (8,9), Albunex (10) or Sonazoid (11). Previously, we developed "Bubble liposomes (BL)" as a novel gene-delivery carrier and reported that the combination of BL and high-frequency US was an effective gene-delivery method *in vitro* and *in vivo* (12–14). We postulate that when BL are exposed to US, they are destroyed, thereby generating a jet stream by cavitation, and consequently transient pores appear in the membranes of cells, through which extracellular plasmid DNA can enter the cytosol.

The development of gene delivery using US technology may contribute to further advancements in the efficiency and optimization of existing periodontal treatments. Few studies have described gene delivery to periodontal tissues, and the development of periodontal gene therapy may provide a new treatment strategy in the future. Therefore, we investigated whether it was possible to deliver genes to the gingiva, which is a typical periodontal tissue and the site of periodontal inflammation, by our transfection system using BL and US.

Material and methods

Animals

Seven-week-old male Wistar rats (Tokyo Laboratory Animals Science, Tokyo, Japan) were used for all animal experiments. All studies were approved by the Animal Experiment Committee of Tokyo University of Pharmacy and Life Sciences. Rats were given feed and tap water *ad libitum* throughout the experimental period.

Preparation of BL

BL were prepared using a previously described method (12,13). In brief, polyethylene glycol liposomes, composed of 1,2-dipalmitoyl-*sn*-glycero-3-phosphocholine (DPPC) (NOF Corporation, Tokyo, Japan) and 1,2-distearoyl-*sn*-glycero-3-phosphatidylethanolamine-polyethyleneglycol (DSPE-PEG_{2000}-OMe) (NOF Corporation), at a molar ratio of 94 : 6, were prepared using a reverse-phase evaporation method. All reagents were dissolved in chloroform/diisopropyl ether (1 : 1; vol/vol). Phosphate-buffered saline was added to the lipid solution, and the mixture was sonicated and then evaporated at 47°C. Then, the organic solvent was completely removed, and the size of the liposomes was adjusted to less than 200 nm using extruding equipment and a sizing filter (pore size = 200 nm) (Nuclepore Track-Etch Membrane, Whatman plc, Maidstone, UK). Lipid concentrations were measured using the Phospholipids C test (Wako Pure Chemical Industries Ltd., Osaka, Japan), and BL were prepared from liposomes and perfluoropropane gas (Takachio Chemical Ind. Co. Ltd., Tokyo, Japan). First, 2-mL sterilized vials containing 0.8 mL of a liposome suspension (lipid concentration = 1 mg/mL) were filled with perfluoropropane gas, capped and then pressurized with a further 3 mL of perfluoropropane gas. The vial was placed in a bath-type sonicator (42 kHz, 100 W) (BRANSONIC 2510j-DTH; Branson Ultrasonics Co., Danbury, CT, USA) for 5 min to form BL.

Plasmid DNA

Two reporter plasmids were used in this study. The pcDNA3-Luc plasmid, which is derived from pGL3-basic (Promega, Madison, WI, USA), is an expression vector that encodes the firefly luciferase gene under the control of the cytomegalovirus promoter. The pCAG-EGFP plasmid (provided by NEPA GENE, Co. Ltd., Chiba, Japan) is an expression vector encoding enhanced green fluorescent protein (EGFP) under the control of the CAG promoter. The CAG promoter is a

hybrid promoter of cytomegalovirus enhancer element and chicken beta-actin promoter, and is frequently used to drive high levels of gene expression in mammalian expression vectors.

In-vivo gene delivery using BL and US

Wistar rats were anesthetized with 40 mg/mL of pentobarbital throughout each procedure via intra-abdominal injection. The limbs and head of each rat were fixed on an original flat board, and the labial gingiva was clearly exposed for the gene-transfection procedure by eversion of the lower lip. A 10-μL mixture of pDNA (10 μg) and BL (5 μg) was injected into the labial gingiva of the incisor in the lower jaw using a 33-gauge syringe (HAMILTON COMPANY, Reno, NV, USA) and US was immediately applied to the injection site. A Sonitron 2000 (NEPA GENE, Co. Ltd) was used as an ultrasound generator, which had a US probe of 6 mm in diameter. US conditions were as follows: frequency, 1 MHz; duty, 50%; intensity, 0–4 W/cm^2; time, 0–120 s.

Measurement of luciferase activity

Several days after the injection, the rats were killed by overdose of anesthesia, and the gingival tissue in the US-exposed area was collected and homogenized with a POLYTRON (KINEMATICA, INC., New York, NY, USA). The cell lysate and tissue homogenates were diluted with lysis buffer [0.1 M Tris–HCl (pH 7.8), 0.1% Triton X-100 and 2 mM EDTA]. Luciferase activity was then measured using a luciferase assay system (Promega) and a luminometer (LB96V; Belthold Japan Co. Ltd., Tokyo, Japan). Activity was indicated as relative light units per mg of protein.

Histological observation of EGFP expression and local cell viability

To identify transfected cells, the mandible, including the incisors and surrounding gingival tissues, was dissected 1 d after the gene-delivery procedure. Dental samples were fixed with 4% paraformaldehyde in phosphate-buffered saline, decalcified with 10% EDTA and embedded in optimal cutting temperature compound. Then, 10-μm-thick frozen sections were cut using a cryostat and EGFP-expressing cells were observed using a fluorescence microscope (Axiovert 200M; Carl Zeiss, Tokyo, Japan). In parallel, serial vertical sections in which EGFP expression was observed were also cut, and hematoxylin and eosin staining was carried out. Microscopy (BZ-8100; KEYENCE, Osaka, Japan) of hematoxylin and eosin-stained specimens was used for morphological observations and for assessing tissue damage. Then, the dental samples were stained with NADH tetrazolium reductase to assess cytotoxicity of US-mediated gene delivery. NADH tetrazolium reductase staining was performed as described in a previous study (15). In brief, 8-μm cryosections were prepared then incubated in a solution of Tris–HCl buffer, Nitro blue tetrazolium (NBT) (Wako Pure Chemical Industries Ltd.) and β-NADH (Wako) at 37°C for 60 min. The sections were then immersed in serial acetone solutions at the concentrations 30%, 60%, 90%, 60% and 30%, washed with deionized H_2O, then mounted with aqueous medium.

Statistical analysis

All data are shown as mean ± SD (n = 5). The Mann–Whitney U-test was used to determine the significance of any differences. Differences detected in multiple comparison tests were assessed using a two-way repeated-measures ANOVA. Differences associated with a $p < 0.05$ were considered significant.

Results

We first attempted to deliver naked pDNA into rat gingival tissue using BL and US under the conditions described in our previous study, in which naked pDNA was delivered into the tongue tissue of mice (16). To optimize the US conditions for *in-vivo* gene delivery into gingival tissue, we examined the US intensity and US exposure time. These US parameters represent two factors that decide the efficiency of delivery. US intensity ranged between 0 and 4.0 W/cm^2. Relative luciferase activity was significantly higher in groups treated at a US intensity of 2.0 W/cm^2 than in the group not exposed to US (Fig. 1A). A slight increase in luciferase intensity was also observed at US intensities of 0.5 and 4.0 W/cm^2. We also examined the effect of US exposure time on transfection efficiency. The highest luciferase activity was observed at a US exposure time of 30 s. Delivery efficiency did not increase in a time-dependent manner, and high activity was maintained until 120 s (Fig. 1B).

Next, we examined the duration of gene expression induced after treatment with BL and US exposure. High luciferase activity was observed 1 d after gene transfection. Lower luciferase activity was observed at subsequent time points, and the lowest luciferase activity was observed 7 d after gene delivery (Fig. 2).

From these results, we decided that the optimal US conditions of gene delivery to the gingiva were US intensity of 2.0 W/cm^2 and US exposure time of 30 s. To assess the combined effect of BL and US, rats were treated under these optimized conditions. Significantly higher gene expression was confirmed in the group treated with BL and US exposure than in the group treated with pDNA alone (Fig. 3). Relative luciferase activity in the group treated with pDNA+BL remained as low as that of the pDNA-only group. In contrast, luciferase activity was slightly higher in the pDNA+US group than in the pDNA-only or pDNA+BL groups.

We also attempted to identify transfected cells by analyzing EGFP expression using fluorescence microscopy. The number of EGFP-expressing cells was higher in gingival tissue treated with BL and US than in the other treatment groups (data not shown). The majority of EGFP-expressing cells were concentrated in the vicinity of the midline of the transfected area. Some sporadic cells expressed EGFP in the connective tissue of the gingiva in the other treat-

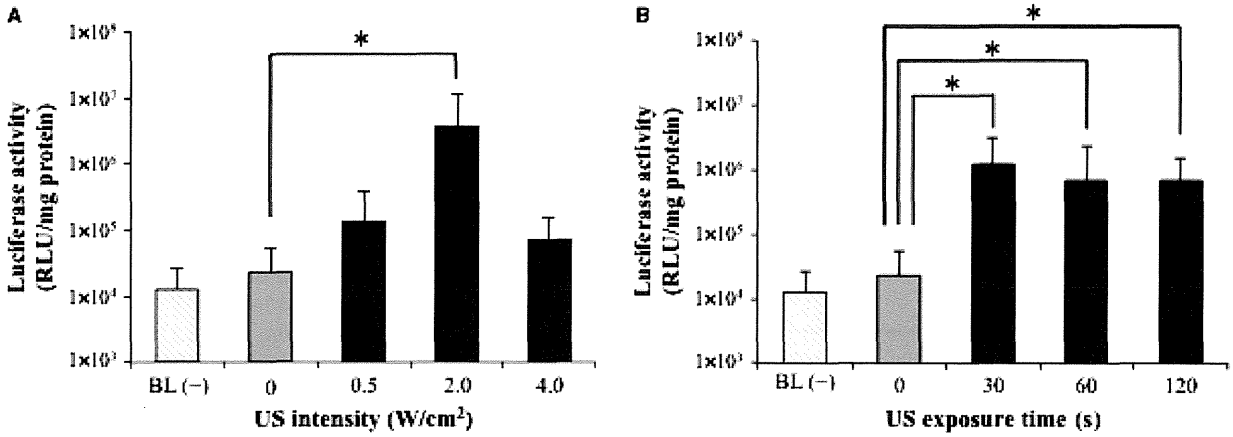

Fig. 1. Characteristics of the ultrasound (US) gene-delivery system using Bubble liposomes (BL). To examine the optimal parameters for BL and US-mediated gene delivery into gingival tissue, rats were subjected to alterations of two US conditions: the US intensity and the US exposure time. The other transfection conditions were as follows: pDNA (pCMV-Luciferase), 10 μg; BL, 5 μg; US frequency, 1 MHz; duty, 50%. Relative luciferase activity activity [measured as relative light units (RLU)] was determined 1 d after transfection. Data are shown as mean ± SD. The BL (-) group was injected with a mixture of pDNA and 5 μl of phosphate-buffered saline instead of with BL. (A) Variations in the gene-expression levels induced by changes in the US intensity. US intensity was set at 0, 0.5, 2.0 or 4.0 W/cm^2. US duration was set at 30 s. *$p < 0.05$, Mann–Whitney U-test ($n = 5$), significantly different from 0 W/cm^2 (no US exposure). (B) Variations in the gene-expression levels induced by changes in the US exposure time. US intensity was set at 2.0 W/cm^2. US duration was set at 0, 30, 60 or 120 s. *$p < 0.05$, Mann–Whitney U-test ($n = 5$), significantly different from 0 s (no US exposure).

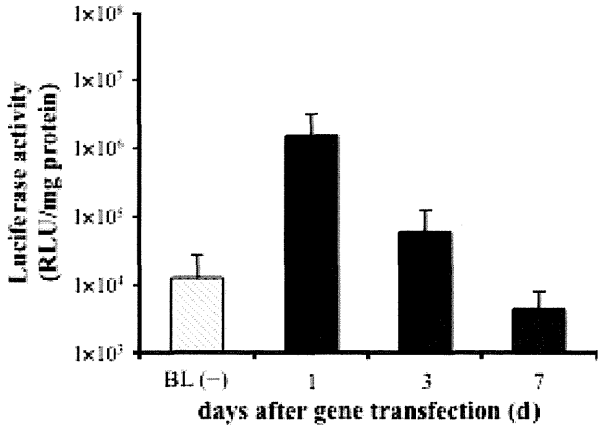

Fig. 2. Duration of gene expression in gingival tissue transfected using Bubble liposomes (BL) and ultrasound (US). Relative luciferase activity [measured as relative light units (RLU)] was examined 1, 3 and 7 d after gene transfection. Transfection conditions were as follows: pDNA (pCMV-Luciferase), 10 μg; BL, 5 μg; and US conditions were: frequency, 1 MHz; duty cycle, 50%; intensity, 2.0 W/cm^2; and time, 30 s. Data are shown as mean ± SD The BL (−) group was injected with a mixture of pDNA and 5 μl of phosphate-buffered saline instead of BL.

ment groups. We further observed the accumulation of many EGFP-expressing cells in both the gingival epithelium layer and the connective tissue layer when a combination of BL and US exposure was used (Fig. 4). Macroscopic observations of US-exposed areas revealed that inflammatory signs such as redness, swelling or hemorrhage were not observed. Furthermore, hematoxylin and eosin-stained samples showing distinct EGFP expression exhibited no inflammation or bleeding. In all delivery areas, including the gingival epithelium and connective tissue, no signs of cytotoxicity, such as inflammatory cell infiltration, were observed (Fig. S1).

Discussion

The prevalence of periodontal disease is increasing, and morbid conditions are becoming complicated. While the onset and progression of periodontitis is greatly affected by dental biofilms, periodontal disease is a multifactorial disease that arises from the relationships among the pathogen (bacterial), the host and the environment. The immunity of periodontal tissue is diminished for genetic effects in some patients. For example, genetic mutations in cytokines, including interleukin-1 and tumor necrosis factor-alpha, have been partially associated with susceptibility to periodontitis (17,18). Moreover, four kinds of genopathy, namely Papillon–Lefèvre syndrome, Haim–Munk syndrome, Chédiak–Higashi syndrome and cyclic neutropenia, have exhibited signs of periodontitis as a result of the dysfunction of a single gene. Therefore, an extensive approach against the individual processes of development and risk factors is required for effective periodontal treatment.

Gene delivery is an innovative approach used to regulate a gene causing a disease and can consequently

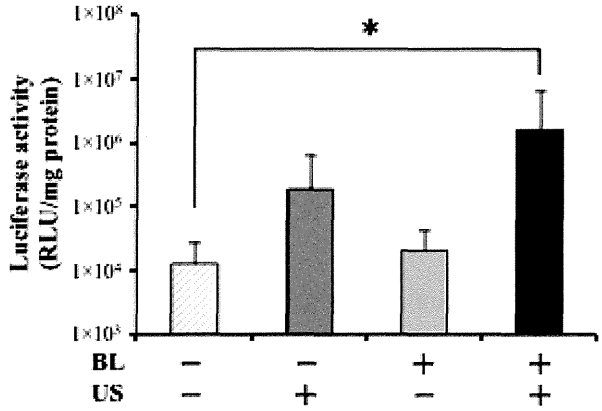

Fig. 3. Luciferase activity in gingival tissue transfected using Bubble liposomes (BL) and ultrasound (US) under optimized conditions. Rats were treated with BL and US-mediated luciferase gene delivery. Relative luciferase activity [measured as relative light units (RLU)] was determined 1 d after transfection. Data are shown as mean ± SD $*p < 0.05$, Mann–Whitney *U*-test ($n = 5$), significantly different from the group treated with a pDNA injection only. pDNA (pCMV-Luciferase), 10 μg; BL, 5 μg; US conditions: frequency, 1 MHz; duty cycle, 50%; intensity, 2.0 W/cm^2; time, 30 s.

enhance or suppress the generation of target proteins. Two main delivery carriers of genes – viral and nonviral vectors – are currently being used for this purpose. While viral vectors are known to be excellent carriers of genes, they are associated with immunogenicity and carcinogenicity (19–21). Therefore, many researchers have reported physical or chemical methods independent of virus. Since Fechheimer *et al.* (22) first reported the US-mediated gene-delivery technique in 1987, therapeutic US has been used as a convenient device to deliver genes or drugs into target tissues. The application of US provides precise target-directivity, with the delivery effect being observed in the US exposure area only. Thus, therapeutic molecules, such as genes, drugs, peptides or recombinant proteins, can be delivered by local administration into the target tissue with a cavitating jet generated by the physical action of US. Our results showed intense distinct expression of EGFP in the US exposure area, especially in the middle of the injected gingiva. When US is utilized to deliver genes or drugs, we can control the depth of focus and the exposure range by changing the wavelength or intensity. However, these parameters need to be optimized specifically for use in each type of target tissue, because an infinite combination of US parameters has been theoretically suggested.

Recently, transfection efficacy was shown to be enhanced by combining US energy with microbubbles (23–26). Microbubbles are known to serve as artificial cavitation nuclei and reduce the threshold of cavitation generated by US (27). We also developed a unique carrier, BL, and reported that the BL-mediated US gene-delivery system enhanced transfection efficiency both *in vitro* and *in vivo* (12–14,28–31). Chen *et al.* (32) demonstrated gene delivery into the gingiva of mice using original nano/microbubbles and US. They showed that delivery efficiency increased when mice were administered a luciferase gene by nano/microbubbles and US exposure; however, high luciferase activity was observed for 1 d only. Moreover, using histological observations, they showed that the transfected cells in gingival tissues were muscle cells. In our results, expression peaked 1 d after the gene-delivery procedure, and relative luciferase activity decreased after 3 d. A previous report showed that transfection efficiency was higher, and gene expression was longer, with repeated US exposure than with single US exposure (33). To extend the duration of the transfection effect while maintaining treatment efficacy, it may be necessary to repeat the delivery procedure. On the other hand, we previously reported, using the same delivery technique, that gene-transfection efficiency into the tongue tissue of mice was maintained for about 10 d with a single treatment (16). Skeletal muscle is one of the candidate target tissues of gene therapy, and stability and longevity after gene delivery is useful for the treatment of diseases. As the characteristics of the target cell may also affect the duration of gene expression, we need to investigate in detail whether sufficient treatment efficacy can be acquired in gingival tissue by gene delivery with BL and US.

As shown in Fig. 4, distinct EGFP-expressing cells were observed in both the gingival epithelium and the connective tissue layer. As the mixture of BL and plasmid DNA was almost wholly diffused in the injected labial gingiva, it is difficult to distinguish between delivery to epithelial tissue and to connective tissue. Although US may localize the delivery area to a specific part of the whole body, other devices are required to distinguish detailed objects, such as cells. For the delivery of anticancer agents, a study was performed using a more delicate technique involving the modification of targeting peptides on the surface of BL before transfection (34). Modified-BL may improve targeting ability at the cellular level. The type of target tissue and delivery efficiency may be affected by exposure to US energy or by the properties of BL, including size, lipid composition and encapsulating gas. Therefore, optimizing conditions in the BL and for the US-mediated delivery technique are necessary for specific tissues. In this study, we optimized the US parameter (2.0 W/cm^2, 30 s) to enhance the efficiency of delivery into gingival tissue. These optimized conditions show the same tendency also in our previous report (16). The characterization of the target tissue could have been influenced a delivery efficiency. For example, the alveolar bone exists just under the gingiva. As the depth of US propagation is different in soft tissue and hard tissue, the composition of target tissue and adjacent tissue may affect the biological response. Moreover, the heat generated by US

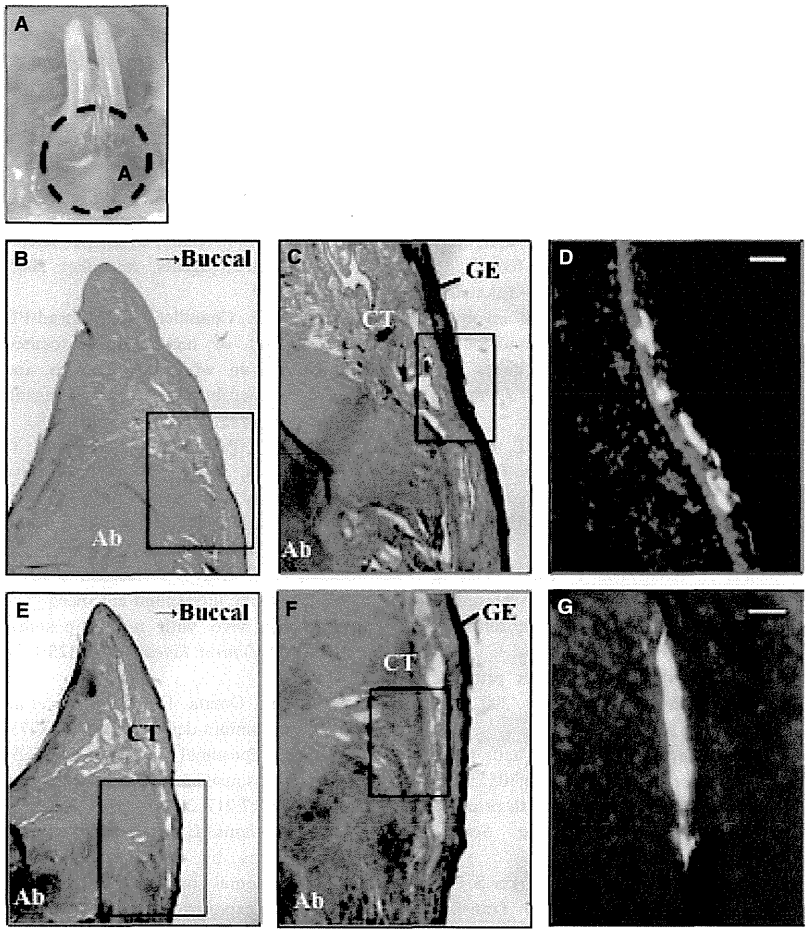

Fig. 4. Localization of enhanced green fluorescent protein (EGFP)-expressing cells. Gingiva treated with Bubble liposomes (BL) and ultrasound (US)-mediated gene delivery were inspected to identify the type of cells that expressed EGFP. Intense EGFP fluorescence was localized in the gingival epithelial layer and the connective tissue layer. No inflammatory cell infiltration was observed in transfected gingival tissues. (A) The transfection area is shown in the dotted line circle. (B, E) Hematoxylin and eosin (H&E) staining in the sagittal sections of rat lower gingiva transfected with BL using US. (C, F) Higher magnifications of B and E (square). (D) EGFP expression in the gingival epithelium layer at a higher magnification of C (square). (G) EGFP expression in the connective tissue layer at a higher magnification of F (square). Blue, DAPI (used for nuclear staining); green, EGFP. Ab, alveolar bone; CT, connective tissue; GE, gingival epithelium. Scale bar: 200 μm.

exposure may cause local tissue damage. Therefore, prolonged US exposure time may lead to decreased transfection efficiency.

Our study is the first to show gene expression in gingival epithelial cells and connective tissue cells, but not in skeletal muscle cells, using a delivery technique combining BL and US. A reporter plasmid was used in this study to examine whether effective gene delivery into the gingiva was achieved when BL and US were used together. Our technique, using BL and US to deliver plasmid DNA into periodontal tissue, is applicable not only for plasmids, but also for peptides, drugs and small interfering RNA. As such molecules have lower molecular mass values than plasmids, transfection may result in deeper penetration of such molecules into tissues, which suggests that our system may be a useful local drug-delivery system for periodontal therapy.

In conclusion, the results of this study demonstrated that the most efficient conditions for US energy for gene delivery into rat gingival tissue using BL and US were US intensity of 2.0 W/cm^2 and US exposure time of 30 s. In the future, our gene-delivery method using BL and US may become a beneficial treatment for patients with periodontitis.

Acknowledgements

We are grateful to Dr Katsuro Tachibana (Department of Anatomy, School of Medicine, Fukuoka University) for his technical advice regarding the induction of cavitation with US, to Mr Yasuhiko Hayakawa and Mr Kosho Suzuki (NEPA GENE Co., Ltd.) for their technical advice regarding US exposure, and to Dr Kenji Mishima (Department of Oral Pathology and Diagnosis, School of Dentistry, Showa University) for his advice regarding histological observation. This study was supported, in part, by the Industrial Technology Research Grant Program (04A05010) from New Energy, the Industrial Technology Development Organization (NEDO) of Japan.

Supporting Information

Additional Supporting Information may be found in the online version of this article:

Figure S1. Histological analysis of local cell viability. Gingival sections (NADH-TR and H&E staining) at higher magnification from rats treated with BL and US-mediated gene delivery. The gingival tissues were examined histologically to assess cytotoxicity. (A): Untreated groups, the gingival epithelium area (a, b) and the connective tissue area (c, d). (B): BL+US groups, the gingival epithelium area (e, f) and the connective tissue area (g, h). pDNA (pCAG-EGFP): 10 μg; BL: 5 μg; US conditions: Frequency: 1 MHz, Duty cycle: 50%, Intensity: 2.0 W/cm^2, Time: 30 s. BL, Bubble liposomes; US, Ultrasound. Scale bar: 50 μm.

References

1. Minabe M, Suzuki F, Umemoto T. Intra-pocket antibiotic therapy using resorbable and non-resorbable slow-

release devices containing tetracycline. *Periodontal Clin Investig* 2000;**22**:14–21.
2. Zetterstrom O, Andersson C, Eriksson L *et al.* Clinical safety of enamel matrix derivative (EMDOGAIN) in the treatment of periodontal defects. *J Clin Periodontol* 1997;**24**:697–704.
3. Bunyaratavej P, Wang HL. Collagen membranes: a review. *J Periodontol* 2001;**72**:215–229.
4. Andreadis ST, Geer DJ. Biomimetic approaches to protein and gene delivery for tissue regeneration. *Trends Biotechnol* 2006;**24**:331–337.
5. Chen FM, An Y, Zhang R, Zhang M. New insights into and novel applications of release technology for periodontal reconstructive therapies. *J Control Release* 2011;**149**:92–110.
6. Lavon I, Kost J. Ultrasound and transdermal drug delivery. *Drug Discov Today* 2004;**9**:670–676.
7. Mitragotri S, Kost J. Low-frequency sonophoresis: a noninvasive method of drug delivery and diagnostics. *Biotechnol Prog* 2000;**16**:488–492.
8. Taniyama Y, Tachibana K, Hiraoka K *et al.* Development of safe and efficient novel nonviral gene transfer using ultrasound: enhancement of transfection efficiency of naked plasmid DNA in skeletal muscle. *Gene Ther* 2002;**9**:372–380.
9. Taniyama Y, Tachibana K, Hiraoka K *et al.* Local delivery of plasmid DNA into rat carotid artery using ultrasound. *Circulation* 2002;**105**:1233–1239.
10. Greenleaf WJ, Bolander ME, Sarkar G, Goldring MB, Greenleaf JF. Artificial cavitation nuclei significantly enhance acoustically induced cell transfection. *Ultrasound Med Biol* 1998;**24**:587–595.
11. Numata K, Luo W, Morimoto M *et al.* Contrast enhanced ultrasound of hepatocellular carcinoma. *World J Radiol* 2010;**2**:68–82.
12. Suzuki R, Takizawa T, Negishi Y *et al.* Gene delivery by combination of novel liposomal bubbles with perfluoropropane and ultrasound. *J Control Release* 2007; **117**:130–136.
13. Negishi Y, Endo Y, Fukuyama T *et al.* Delivery of siRNA into the cytoplasm by liposomal bubbles and ultrasound. *J Control Release* 2008;**132**:124–130.
14. Negishi Y, Matsuo K, Endo-Takahashi Y *et al.* Delivery of an angiogenic gene into ischemic muscle by novel bubble liposomes followed by ultrasound exposure. *Pharm Res* 2011;**28**:712–719.
15. Sachchida NP, Jennifer C, Rongye S *et al.* Conditional over-expression of PITX1 causes skeletal muscle dystrophy in mice. *Biol Open* 2012;**1**:629–639.
16. Sugano M, Negishi Y, Endo-Takahashi Y *et al.* Gene delivery system involving Bubble liposomes and ultrasound for the efficient in vivo delivery of genes into mouse tongue tissue. *Int J Pharm* 2012;**422**:332–337.
17. Loos BG, John RP, Laine ML. Identification of genetic risk factors for periodontitis and possible mechanisms of action. *J Clin Periodontol* 2005;**32**(suppl 6):159–179.
18. Yoshie H, Kobayashi T, Tai H, Galicia JC. The role of genetic polymorphisms in periodontitis. *Periodontol* 2000;**2007**(43): 102–132.
19. Check E. Safety panel backs principle of gene-therapy trials. *Nature* 2002;**420**: 595.
20. Check E. Second cancer case halts gene-therapy trials. *Nature* 2003;**421**:305.
21. Marshall E. Gene therapy death prompts review of adenovirus vector. *Science* 1999;**286**:2244–2245.
22. Fechheimer M, Boylan JF, Parker S, Sisken JE, Patel GL, Zimmer SG. Transfection of mammalian cells with plasmid DNA by scrape loading and sonication loading. *Proc Natl Acad Sci USA* 1987;**84**:8463–8467.
23. Alter J, Sennoga CA, Lopes DM, Eckersley RJ, Wells DJ. Microbubble stability is a major determinant of the efficiency of ultrasound and microbubble mediated in vivo gene transfer. *Ultrasound Med Biol* 2009;**35**:976–984.
24. Hassan MA, Feril LB Jr, Suzuki K, Kudo N, Tachibana K, Kondo T. Evaluation and comparison of three novel microbubbles: enhancement of ultrasound-induced cell death and free radicals production. *Ultrason Sonochem* 2009;**16**:372–378.
25. Li T, Tachibana K, Kuroki M. Gene transfer with echo-enhanced contrast agents: comparison between Albunex, Optison, and Levovist in mice–initial results. *Radiology* 2003;**229**:423–428.
26. Wang X, Liang HD, Dong B, Lu QL, Blomley MJ. Gene transfer with microbubble ultrasound and plasmid DNA into skeletal muscle of mice: comparison between commercially available microbubble contrast agents. *Radiology* 2005; **237**:224–229.
27. Poliachik SL, Chandler WL, Mourad PD *et al.* Effect of high-intensity focused ultrasound on whole blood with and without microbubble contrast agent. *Ultrasound Med Biol* 1999;**25**:991–998.
28. Suzuki R, Takizawa T, Negishi Y, Utoguchi N, Maruyama K. Effective gene delivery with novel liposomal bubbles and ultrasonic destruction technology. *Int J Pharm* 2008;**354**:49–55.
29. Suzuki R, Takizawa T, Negishi Y *et al.* Tumor specific ultrasound enhanced gene transfer in vivo with novel liposomal bubbles. *J Control Release* 2008;**125**:137–144.
30. Negishi Y, Omata D, Iijima H *et al.* Enhanced laminin-derived peptide AG73-mediated liposomal gene transfer by bubble liposomes and ultrasound. *Mol Pharm* 2010;7:217–226.
31. Suzuki R, Namai E, Oda Y *et al.* Cancer gene therapy by IL-12 gene delivery using liposomal bubbles and tumoral ultrasound exposure. *J Control Release* 2010;**142**:245–250.
32. Chen R, Chiba M, Mori S, Fukumoto M, Kodama T. Periodontal gene transfer by ultrasound and nano/microbubbles. *J Dent Res* 2009;**88**:1008–1013.
33. Bekeredjian R, Chen S, Frenkel PA, Grayburn PA, Shohet RV. Ultrasound-targeted microbubble destruction can repeatedly direct highly specific plasmid expression to the heart. *Circulation* 2003;**108**:1022–1026.
34. Hamano N, Negishi Y, Omata D *et al.* Bubble liposomes and ultrasound enhance the antitumor effects of AG73 liposomes encapsulating antitumor agents. *Mol Pharm* 2012;**10**:774–779.

Journal of Thrombosis and Haemostasis, **11**: 1565–1573 DOI: 10.1111/jth.12321

ORIGINAL ARTICLE

Thrombus-targeted perfluorocarbon-containing liposomal bubbles for enhancement of ultrasonic thrombolysis: *in vitro* and *in vivo* study

K. HAGISAWA,* T. NISHIOKA,† R. SUZUKI,‡ K. MARUYAMA,‡ B. TAKASE,§ M. ISHIHARA,§ A. KURITA,§ N. YOSHIMOTO,† Y. NISHIDA,* K. IIDA,¶ H. LUO¶ and R. J. SIEGEL¶

**Department of Physiology, National Defense Medical College, Tokorozawa; †Division of Cardiology, Saitama Medical Center, Saitama Medical University, Kawagoe; ‡Department of Drug Delivery System, School of Pharmaceutical Sciences, Teikyo University, Tokyo; §Division of Biomedical Engineering, National Defense Medical College Research Institute, Tokorozawa, Japan; and ¶Cardiac Non-invasive Laboratory, Heart Institute, Cedars-Sinai Medical Center, Los Angeles, CA, USA*

To cite this article: Hagisawa K, Nishioka T, Suzuki R, Maruyama K, Takase B, Ishihara M, Kurita A, Yoshimoto N, Nishida Y, Iida K, Luo H, Siegel RJ. Thrombus-targeted perfluorocarbon-containing liposomal bubbles for enhancement of ultrasonic thrombolysis: *in vitro* and *in vivo* study. *J Thromb Haemost* 2013; **11**: 1565–73.

Summary. *Background:* External low-frequency ultrasound (USD) in combination with microbubbles has been reported to recanalize thrombotically occluded arteries in animal models. *Objective:* The purpose of this study was to examine the enhancing effect of thrombus-targeted bubble liposomes (BLs) developed for fresh thrombus imaging during ultrasonic thrombolysis. *Methods: In vitro*: after the administration of thrombus-targeted BLs or non-targeted BLs, the clot was exposed to low-frequency (27 kHz) USD for 5 min. *In vivo*: Rabbit iliofemoral arteries were thrombotically occluded, and an intravenous injection of either targeted BLs ($n = 22$) or non-targeted BLs ($n = 22$) was delivered. External low-frequency USD (low intensity, 1.4 W cm^{-2}, to 12 arteries, and high intensity, 4.0 W cm^{-2}, to 10 arteries, for both the targeted BL group and the non-targeted BL group) was applied to the thrombotically occluded arteries for 60 min. In another 10 rabbits, recombinant tissue-type plasminogen activator (rt-PA) was intravenously administered. *Results: In vitro*: the weight reduction rate of the clot with targeted BLs was significantly higher than that of the clot with non-targeted BLs. *In vivo*: TIMI grade 3 flow was present in a significantly higher number of rabbits with USD and targeted BLs than rabbits with USD and non-targeted BLs, or with rt-PA monotherapy. High-intensity USD exposure with targeted BLs achieved arterial recanalization in 90% of arteries, and the time to reperfusion was shorter than with rt-PA treatment (targeted BLs, 16.7 ± 5.0 min; rt-PA, 41.3 ± 14.4 min). *Conclusions:* Thrombus-targeted BLs developed for USD thrombus imaging enhance ultrasonic disruption of thrombus both *in vitro* and *in vivo*.

Keywords: drug targeting, liposomes, RGD peptide, thrombolytic therapy, ultrasound.

Correspondence: Toshihiko Nishioka, Division of Cardiology, Saitama Medical Center, Saitama Medical University, 1981, Kamoda, 350-8550 Kawagoe, Japan.
Tel.: +81 49 228 3587; fax: +81 49 226 5274.
E-mail: nishioka@saitama-med.ac.jp

Received 5 December 2012
Manuscript handled by: R. Medcalf
Final decision: D. Lane, 9 June 2013

Introduction

Most life-threatening cardiovascular events, including acute coronary syndrome and ischemic stroke, are caused by arterial thrombosis. Acute ST-elevation myocardial infarction (STEMI) is characterized by atherosclerotic plaque rupture and occlusive thrombus formation associated with platelet aggregation [1,2]. Percutaneous coronary intervention (PCI) and fibrinolysis are the standard therapeutic strategies for recanalizing thrombotically occluded arteries in patients with STEMI [3]. Primary PCI is performed in most of the STEMI patients presenting to a PCI-capable facility, with a cardiac catheterization laboratory, an interventional cardiologist, and the appropriate specialized staff and equipment to perform acute PCI. Enzymatic fibrinolysis for the treatment of STEMI is less invasive and logistically more convenient; however, this option gives a lower initial recanalization rate, and a higher incidence of coronary reocclusion and life-threatening systemic bleeding, and may result in worse short-term and long-term clinical outcomes than direct PCI [4,5]. For ischemic stroke treatment, fibrinolysis is recommended only for selected patients who can be